Kinetics and thermodynamics of intra- and intermolecular rearrangement in binaphtholate complexes of titanium(IV)

Timothy J. Boyle, Denise L. Barnes, Joseph A. Heppert,
Luis Morales, Fusao Takusagawa, and John C. Connolly

More About This Article

The permalink http://dx.doi.org/10.1021/om00039a017 provides access to:

- Links to articles and content related to this article
- Copyright permission to reproduce figures and/or text from this article

Kinetics and Thermodynamics of Intra- and Intermolecular Rearrangement in Binaphtholate Complexes of Titanium(IV)

Timothy J. Boyle, Denise L. Barnes, Joseph A. Heppert,* Luis Morales, and Fusao Takusagawa

Department of Chemistry, University of Kansas, Lawrence, Kansas 66045†

John W. Connolly

Department of Chemistry, University of Missouri—Kansas City, Kansas City, Missouri 64110

Received August 21, 1991

3,3′-Disubstituted-1,1′-bi-2-naphthols (H_2R_2BINO where R = Me or $SiMe_2$-t-Bu) react with $Ti(O\text{-}i\text{-}Pr)_4$ to produce molecules of empirical formula $[(R_2BINO)Ti(O\text{-}i\text{-}Pr)_2]_n$. Analytical methods including NMR spectroscopy, molecular weight cryoscopy, and X-ray crystallography were used to identify the (t-$BuMe_2Si)_2BINO$-substituted complex as a monomer and the Me_2BINO-substituted complex as a dimer. This dinuclear complex possesses a highly distorted edge-fused trigonal-bipyramidal structure, whose 1,3-Ti_2O_2 core is bridged by two naphthoxide units. There is a distinct thermodynamic preference for the incorporation of ligands of like chirality into the dimer. A second set of complexes having empirical formula $(R_2BINO)Ti_2(O\text{-}i\text{-}Pr)_6$ (R = Me, $SiMe_2$-t-Bu) are accessible through either the reaction of 2 equiv of $Ti(O\text{-}i\text{-}Pr)_4$ with H_2R_2BINO or a reaction between $[(R_2BINO)Ti(O\text{-}i\text{-}Pr)_2]_n$ and $Ti(O\text{-}i\text{-}Pr)_4$. The $(Me_2BINO)Ti_2(O\text{-}i\text{-}Pr)_6$ complex possesses C_1 symmetry at the low-temperature limit, implying that the molecule adopts an edge-fused trigonal-bipyramidal structure bridged by one naphthoxide and one isopropoxide ligand. At higher temperatures, a fluxional process, ($\Delta G^{\ddagger}_{240}$ = 10.8 kcal/mol) generates time-averaged C_2 symmetry consistent with the rupture of the isopropoxide bridge to produce a binaphtholate ligand bound to two "$Ti(O\text{-}i\text{-}Pr)_3$" units. $\{(t\text{-}BuMe_2Si)_2BINO\}Ti_2(O\text{-}i\text{-}Pr)_6$ adopts this C_2-symmetric structure in both solution and the solid state. Both the $(Me_2BINO)Ti_2(O\text{-}i\text{-}Pr)_6$ and $\{(t\text{-}BuMe_2Si)_2BINO\}Ti_2(O\text{-}i\text{-}Pr)_6$ complexes display temperature-dependent equilibria in solution between $Ti(O\text{-}i\text{-}Pr)_4$ and either $[(Me_2BINO)Ti(O\text{-}i\text{-}Pr)_2]_2$ or $\{(t\text{-}BuMe_2Si)_2BINO\}Ti(O\text{-}i\text{-}Pr)_2$, respectively. The thermodynamic characteristics of these equilibria follow: Me_2BINO, ΔH° = -12.5 ± 0.6 kcal/mol, ΔS° = 38 ± 2 eu; $(t\text{-}BuMe_2Si)_2BINO$, ΔH° = -12.0 ± 0.8 kcal/mol, ΔS° = -44 ± 4 eu. The $(Me_2BINO)Ti_2(O\text{-}i\text{-}Pr)_6$ complex also engages in an independent intermolecular exchange processes in which a "$Ti(O\text{-}i\text{-}Pr)_4$" unit is exchanged with free $Ti(O\text{-}i\text{-}Pr)_4$ in solution ($\Delta H^{\ddagger}$ = 14.1 ± 0.9 kcal/mol, $\Delta S^{\ddagger}$ = -2 ± 2 eu). When compared with the previously observed fluxional process in $(Me_2BINO)Ti_2(O\text{-}i\text{-}Pr)_6$, this observation demonstrates that polynuclear titanium complexes can engage in distinct intramolecular and intermolecular exchange processes. Crystal data for $\{(t\text{-}BuMe_2Si)_2BINO\}Ti(O\text{-}i\text{-}Pr)_2$ at 113 K: a = 10.866 (3) Å, b = 15.572 (4) Å, c = 23.059 (4) Å, β = 93.76 (2)°, Z = 4, D_{calc} = 1.152, space group $P2_1/c$, R(F) = 0.037, $R_w(F)$ = 0.051 for 3861 reflections. Crystal data for $[(Me_2BINO)Ti(O\text{-}i\text{-}Pr)_2]_2$ at 106 K: a = 17.728 (3) Å, b = 11.079 (4) Å, c = 26.232 (4) Å, β = 101.00 (3)°, Z = 4, D_{calc} = 1.257, space group $P2_1/c$, R(F) = 0.069, $R_w(F)$ = 0.077 for 3231 reflections. Crystal data for $\{(t\text{-}BuMe_2Si)_2BINO\}Ti_2(O\text{-}i\text{-}Pr)_6$ at 113 K: a = 14.444 (2) Å, b = 18.676 (3) Å, c = 20.788 (4) Å, β = 98.76 (2)°, Z = 4, D_{calc} = 1.143, space group $C2/c$, R(F) = 0.059, $R_w(F)$ = 0.091 for 2860 reflections.

Introduction

Over the past 15 years, the use of titanium complexes containing alkoxide ligands as reagents and catalysts for organic synthesis has undergone rapid development. Titanium alkoxide reagents have been applied as templates for chelation-controlled stereoselective nucleophilic addition to ketones[1,2] and as alternatives to alkyllithium and Grignard reagents in chemoselective alkylation processes.[3] Catalysts derived from titanium and other group 4 alkoxides have been used in 2 + 2 and 2 + 3 cycloaddition reactions,[4] trans-esterification processes,[5,6] the polymerization of olefins,[7] and the epoxidation of allylic alcohols.[8,9] More recently, studies of titanium complexes incorporating chiral alcoholate ligands such as dialkyl tartrates,[10,11] disaccharides,[12] and binaphthols[13,14] have led to a range of new enantiospecific reagents and catalysts for alkyl transfer,[12-14] epoxidation,[10,11] aldol condensation,[12] other electrocyclization reactions,[12,13] and molecular recognition studies.[15] As the scope of synthetic applications of titanium alkoxide complexes has expanded, so too has their significance in the repertoire of synthetic organic chemists.

But the complexity of titanium alkoxide coordination chemistry has contributed a substantial degree of uncertainty to the identity of catalytically active species in many such systems.[16,17] Part of this difficulty stems from the

rapidity of intra- and intermolecular ligand and Ti fragment exchange, which frequently raises questions about

(1) (a) Seebach, D.; Prelog, V. *Angew. Chem., Int. Ed. Engl.* 1982, *21*, 654. (b) Seebach, D.; Widler, L. *Helv. Chim. Acta* 1982, *65*, 1972. (c) Weidmann, B. Seebach, D.; Widler, A. G.; Olivero, A. G.; Maycock, D. G.; Seebach, D. *Helv. Chim. Acta* 1981, *64*, 357. (d) Seebach, D. In *Modern Synthetic Methods*; Scheffold, R., Ed.; Wiley: New York; Vol. 3, pp 217-353. (e) Olivero, A. G.; Weidmann, B.; Seeback, D. *Helv. Chim. Acta* 1981, *64*, 2485.
(2) (a) Reetz, M. T.; Kessler, K. Schmidtberger, S.; Wenderoth, B.; Steinback, R. *Angew. Chem., Int. Ed. Engl.* 1983, *22*, 1989. (b) Reetz, M. L. In *Current Topics in Chemistry*; Boschke, F. L., Ed.; Springer Verlag: New York, 1982; Vol. 3, 106, pp 3-54. (c) Reetz, M. T.; Westermann, J.; Steinbach, R. *Angew. Chem.* 1980, *92*, 931. (d) Reetz, M. T.; Wenderoth, R.; Peter, R.; Steinbach, J.; Westermann, J. *J. Chem. Soc., Chem. Commun.* 1980, 1202. (f) Reetz, M. T.; Werderoth, B.; Steinbach, R. *Synth. Commun.* 1981, *11*, 261.
(3) (a) Weidmann, B. Seebach, D.; Widler, A. G.; Olivero, A. G.; Maycock, D. G.; Seebach, D. *Helv. Chim. Acta* 1981, *64*, 357. (b) Tomioka, K. *Synthesis* 1990, 541.
(4) (a) Narasaka, K. *Synthesis* 1990, 1. (b) Engler, T. A.; Combrink, K. D.; Ray, J. E. *J. Am. Chem. Soc.* 1988, *110*, 7931.
(5) Weidmann, B.; Seebach, D. *Angew. Chem., Int. Ed. Engl.* 1983, *22*, 31. (b) Seebach, D.; Hungerburhler, E.; Naef, R.; Schnurrenberger, P.; Weidmann, B.; Zuger, M. F. *Synthesis* 1982, 138.
(6) (a) Rehwinkel, H.; Steglich, W. *Synthesis* 1982, 826. (b) Marsi, M. *Inorg. Chem.* 1988, *27*, 3067.
(7) (a) Burkhardt, T. J.; Funk, W.; Langer, A. W.; Steiger, J. J. *Abstracts of Papers*, 196th National Meeting of the American Chemical Society, Los Angeles, CA, Sept 1988; American Chemical Society: Washington, DC, 1988; Abstr. 364. (b) Masi, F.; Malquori, S. Barazzoni, L.; Ferrero, C.; Moalli, A.; Marconi, F.; Invernizzi, R.; Zandora, N.; Altomare, A.; Ciardelli, F. *Makromol. Chem. Suppl.* 1989, *15*, 147.
(8) Sharpless, K. B.; *Pure Appl. Chem.* 1983, *55*, 1823.

whether structurally characterized solid-state species are actually the active catalyst present in the solution phase. The propensity of formally tetravalent group 4 complexes containing alkoxide ligands to exist as a temperature and concentration dependent equilibrium mixture of polynuclear oligomers further complicates the task of identifying the actual molecular species participating in many chemical processes.[19,20] A prototypical example of the importance of overcoming these challenges in order to develop a link between catalyst structure and the enantioselectivity of a catalytic reaction can be seen in the study of the Sharpless epoxidation catalyst, [(dialkyl tartrate)Ti(O-*i*-Pr)$_2$]$_2$.[19]

Unlike the Sharpless catalyst, other synthetically important titanium-based catalysts, including some that contain simple alkoxide ligands and some that contain alternative diolate chiral auxiliaries, suffer from a virtual lack of information about the structural characteristics imposed by the alkoxide ligands. Furthermore, many catalysts of this type still lack a systematic treatment of such fundamental subjects as (1) the types of rearrangement pathways available for a particular polynuclear alkoxide moiety, (2) the detailed mechanisms of intermolecular and intramolecular rearrangement processes, (3) the relative rates of intra- and intermolecular rearrangement pathways, and (4) the thermodynamics of equilibria involving polynuclear alkoxide complexes. This information, were it more readily available, could act as a guide for synthetic chemists in the design and assessment of new titanium alkoxide reagents and catalysts.

Our interests in this area have focused on the coordination chemistry of 1,1′-bi-2-naphtholate[21,22] complexes of groups 4–6 elements, as a prelude to applying binaphtholate (R$_2$BINO) substituted organo-transition-metal reagents in stereospecific reactions.[23] During the char-

acterization of a series of simple "(R$_2$BINO)Ti(O-*i*-Pr)$_2$" derivatives, we encountered a range of complexes having unusually spectroscopically tractable intra- and intermolecular rearrangement processes. Through both spectroscopic and structural studies, we have succeeded in outlining far more of the fundamental coordination chemistry of the R$_2$BINO auxiliary than was previously known. In this paper we report some of the results of our studies, which include the examples of readily spectroscopically characterizable equilibria between well-defined titanium alkoxide complexes and a detailed study of the kinetics of competing intra- and intermolecular exchange pathways in dinuclear titanium alkoxide/aryloxide complexes.

Results

Synthesis and Characterization of (R$_2$BINO)Ti(O-*i*-Pr)$_2$ Derivatives. Reactions between stoichiometric quantities of racemic 3,3′-disubstituted binaphthol (*rac*-H$_2$R$_2$BINO) and Ti(O-*i*-Pr)$_4$ produce compounds of empirical formula (R$_2$BINO)Ti(O-*i*-Pr)$_2$, with concomitant elimination of 2 equiv of *i*-PrOH (eq 1). The products are isolated as bright yellow-orange crystalline materials from cold ether or hexanes. Derivatives prepared from H$_2$Me$_2$BINO[21a] and H$_2$(*t*-BuMe$_2$Si)$_2$BINO[21b] are significantly easier to isolate as analytically pure materials than corresponding BINO and Ph$_2$BINO complexes.[24,25]

$$n\text{Ti(O-}i\text{-Pr)}_4 + n\text{H}_2\text{R}_2\text{BINO} \xrightarrow{-2n\,i\text{-PrOH}} [(\text{R}_2\text{BINO})\text{Ti(O-}i\text{-Pr)}_2]_n \quad (1)$$
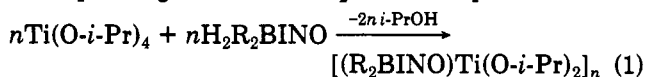
The reaction of 2 equiv of H$_2$R$_2$BINO with Ti(O-*i*-Pr)$_4$ failed to produce a simple homoleptic (R$_2$BINO)$_2$Ti complex. To confirm this assessment, (Me$_2$BINO)$_2$Ti was prepared via halide metathesis between TiCl$_4$ and Li$_2$Me$_2$BINO (eq 2).[24] Unlike the yellow (Me$_2$BINO)$_2$Ti product obtained by this method, the material obtained from the alcoholysis reaction was red and possessed a largely featureless ^{1}H NMR spectrum. We have, as yet, not characterized this alcoholysis product.

$$\text{TiCl}_4 + 2\text{Li}_2\text{Me}_2\text{BINO} \xrightarrow{-4\text{LiCl}} (\text{Me}_2\text{BINO})_2\text{Ti} \quad (2)$$
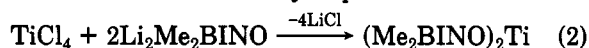
The ^{1}H and ^{13}C NMR spectra of {(*t*-BuMe$_2$Si)$_2$BINO}Ti(O-*i*-Pr)$_2$ are invariant over a wide temperature range and are characteristic of a molecule having rigorous C_2 symmetry. Singular aspects of the proton spectrum include diastereotopic *i*-PrO methyl (δ = 1.14, 1.02) and *t*-BuMe$_2$Si methyl (δ = 0.49, 0.42) resonances. The simplicity and apparent lack of fluxionality in NMR spectra of {(*t*-BuMe$_2$Si)$_2$BINO}Ti(O-*i*-Pr)$_2$ suggest that it could be mononuclear in both solution and the solid state. This assertion is borne out in an X-ray structure of the molecule (vide infra).

NMR spectra of "(Me$_2$BINO)Ti(O-*i*-Pr)$_2$" at the high-temperature limit (Figure 1) are similar to those of the C_2-symmetric {(*t*-BuMe$_2$Si)$_2$BINO}Ti(O-*i*-Pr)$_2$. As the temperature is reduced, each resonance in the spectrum undergoes decoalescence to produce a pair of resonances at a low-temperature limit of 193 K. The pairwise inequivalence of the naphtholate and isopropoxide ligands is consistent with the existence of a dinuclear complex in which the two metals, joined through the agency of either alkoxide or aryloxide bridges, adopt an edge-fused bis-trigonal-bipyramidal coordination environment. Partial confirmation of this hypothesis was obtained through a

(9) (a) Katsuki, T.; Sharpless, K. B. *J. Am. Chem. Soc.* **1980**, *102* 5974. (b) Martin, V. S.; Woodard, S. S.; Katuski, T.; Yamada, Y.; Ikeda, M.; Sharpless, K. B. *J. Am. Chem. Soc.* **1981**, *103*, 6237. (c) Lu, L. D-L.; Johnson, R. A.; Finn, M. G.; Sharpless, K. B. *J. Org. Chem.* **1984**, *49*, 731.

(10) Seebach, D.; Beck, A.; Schiess; Widler, L.; Wonnacott, A. *Pure Appl. Chem.* **1983**, *55*, 1807.

(11) (a) Seebach, D.; Beck, A. K.; Roggo, S.; Wonnacott, A. *Chem. Ber.* **1985**, *118*, 3673. (b) Seebach, D.; Beck, A. K.; Imwinkelreid, R.; Roggo, S.; Wonnacott, A. *Helv. Chim. Acta* **1987**, *70*, 954.

(12) (a) Riediker, M., Duthaler, R. O. *Angew. Chem.* **1989**, *107*, 488. (b) Duthaler, R. O.; Herold, P.; Lottenbach, W.; Oertle, K.; Riediker, M. *Angew. Chem.* **1989**, *101*, 490. (c) Duthaler, R. O.; Riediker, M. *Angew. Chem.* **1989**, *101*, 491. (d) Riediker, M.; Hafner, A.; Piantini, V.; Rihs, G.; Togizi, A. *Angew. Chem.* **1989**, *101*, 493.

(13) (a) Nakai, T.; Terada, M.; Mikami, K. *J. Am. Chem. Soc.* **1989**, *111*, 1940. (b) Mikami, K.; Terada, M.; Nakai, T. *J. Am. Chem. Soc.* **1990**, *192*, 3949.

(14) Reetz, M. L.; Kyung, S.-H.; Bolm, C.; Zierke, T. *Chem. Ind.* **1986**, 824.

(15) Pedersen, S. F.; Hofmeister, G. E. Hahn, F. E. *J. Am. Chem. Soc.* **1989**, *111*, 2319.

(16) Bradley, D. C.; Mehrotra, R. C.; Gaur, D. P. *Metal Alkoxides*; Academic Press: New York, 1978.

(17) Chisholm, M. H.; Rothwell, I. P. In *Comprehensive Coordination Chemistry*; Wilkinson, G., Ed.; Pergammon Press: Oxford, U.K., 1987; Vol. 2, p 335.

(18) (a) Bradley, D. C.; Hollway, C. E. *J. Chem. Soc. A* **1968**, 1316. (b) Hao, N.; Sayer, B. G.; Denes, G.; Bickely, D. G. Detellier, C.; McGlinchey, M. J. *J. Magn. Reson.* **1982**, *50*, 50. (c) Potvin, P. G.; Kwong, P. C. C.; Brook, M. A. *J. Chem. Soc., Chem. Commun.* **1988**, 773. (d) Weingarten, H.; VanWazer, J. R. *J. Am. Chem. Soc.* **1965**, *87*, 724.

(19) Finn, M. B.; Sharpless, K. B. In *Asymmetric Synthesis*; Morrison, J. D., Ed.; Academic Press: New York, 1985; Vol. 5, Chapter 8.

(20) (a) Woodard, S. S.; Finn, M. G.; Sharpless, K. B. *J. Am. Chem. Soc.* **1991**, *113*, 106. (b) Finn, M. G.; Sharpless, K. B. *J. Am. Chem. Soc.* **1991**, *113*, 113.

(21) (a) Lingfelter, D. S.; Hegelson, R. C.; Cram, D. J. *J. Org. Chem.* **1981**, *46*, 393. (b) Maruoka, K.; Itou, T.; Akaki, Y.; Shirasaka, T.; Yamamoto, H. *Bull. Chem. Soc. Jpn.* **1988**, *61*, 2975.

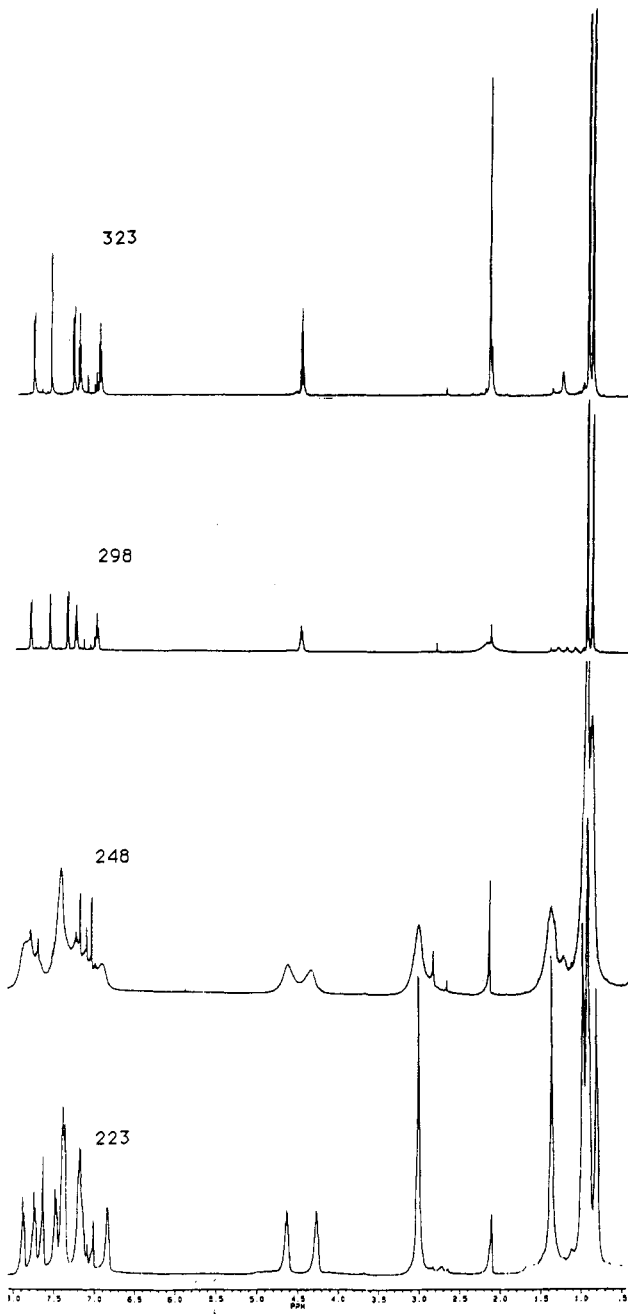(22) Noyori, R.; Suga, S.; Kawai, K.; Okada, S.; Kitamure, M. *Pure Appl. Chem.* **1988**, *60*, 1597.

(23) (a) Heppert, J. A.; Dietz, S. D.; Boyle, T. J.; Takusagawa, F. *J. Am. Chem. Soc.* **1989**, *111*, 1503. (b) Heppert, J. A.; Dietz, S. D.; Eilerts, N. W. *Angew. Chem. Int. Ed. Engl.*, in press.

(24) Boyle, T. J. Ph.D. Thesis, University of Kansas, 1990.

(25) Martin, C. Ph.D. Thesis, M.I.T., 1988. We thank Prof. K. B. Sharpless for access to this reference.

Figure 1. Variable-temperature 500-MHz ^{1}H NMR spectrum of [(Me$_2$BINO)Ti(O-i-Pr)$_2$]$_2$ in toluene-d_8.

cryoscopic molecular weight determination in benzene, which demonstrated that [(Me$_2$BINO)Ti(O-i-Pr)$_2$]$_n$ exists primarily as a dimer in solution (n = 2). Activation parameters for the rearrangement of [(Me$_2$BINO)Ti(O-i-Pr)$_2$]$_2$ (ΔH^* = 14.7 ± 0.4 kcal/mol, ΔS^* = 10.5 ± 2 eu) were obtained from an Eyring plot of the rate constants for exchange, derived from the pairwise coalescence of proton resonances at various temperatures (Figure 2). The activation parameters for this rearrangement process are quite similar to those found for the Sharpless epoxidation catalyst.[20]

The determined nuclearity of [(Me$_2$BINO)Ti(O-i-Pr)$_2$]$_2$ raises some fundamental questions about the structure of this molecule, in that either the isopropoxide or naphtholate ligands could conceivably bridge the dititanium framework. Although we might hypothesize that the more basic i-PrO ligand should form a more thermodynamically stable 1,3-dioxadititanacycle unit, several steric considerations argue against this proposal. First, solutions of
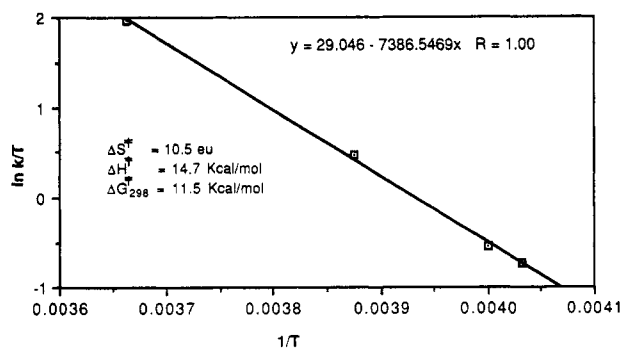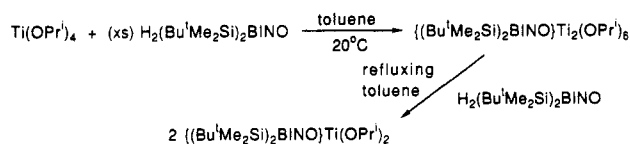

Figure 2. Eyring plot for the rearrangement of [(Me$_2$BINO)-Ti(O-i-Pr)$_2$]$_2$ with rate constants calculated from the pairwise coalescence of various resonances over a range of temperatures. Determined activation parameters include ΔH^* = 14.7 ± 0.4 kcal/mol, ΔS^* = 10 ± 2 eu, and ΔG^*_{298}(calc) = 11.5 kcal/mol.
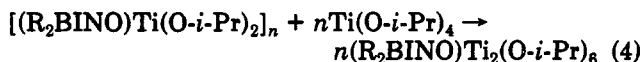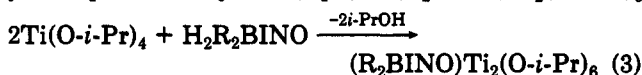
Scheme I

Ti(O-i-Pr)$_4$, having Ti concentrations comparable to those examined in this study, establish a monomer–dimer equilibrium which favors the existence of the monomer near ambient temperature.[26] It is apparently the introduction of a less sterically demanding Me$_2$BINO ligand that facilitates the formation of the [(Me$_2$BINO)Ti(O-i-Pr)$_2$]$_2$ dimer. Second, the bulky i-PrO ligand in a bridging environment would be forced to interact with ligands bound to both metal centers. Unless the destabilizing steric interactions engendered by the i-PrO bridge were outweighed by its additional thermodynamic stability, it seems likely that the binaphtholate ligand would prefer to occupy the bridging site.

Further, we should be drawn to consider the preferred stereochemistry of the [(Me$_2$BINO)Ti(O-i-Pr)$_2$]$_2$ complex. Each of the potential dinuclear structures for [(Me$_2$BINO)Ti(O-i-Pr)$_2$]$_2$ (i.e., Me$_2$BINO-bridged or i-PrO-bridged) can contain naphtholate ligands of the R^*,R^* or unlike R,S stereochemistry. Spectroscopic evidence at the slow-exchange limit is consistent with the existence of only one isomer. Spectra of [(Me$_2$BINO)Ti(O-i-Pr)$_2$]$_2$ prepared from either racemic or optically pure (R)-H$_2$Me$_2$BINO are indistinguishable at the slow-exchange limit in toluene-d_8 and chloroform-d_1. This result provides circumstantial evidence that the R^*,R^* diastereomer is thermodynamically preferred over the R,S isomer in relatively nonpolar solvents.

Synthesis and Characterization of (R$_2$BINO)Ti$_2$-(O-i-Pr)$_6$ Complexes. Reactions between H$_2$R$_2$BINO (R = Me, t-BuMe$_2$Si) and 2 equiv of Ti(O-i-Pr)$_4$ produce complexes of empirical formula (R$_2$BINO)Ti$_2$(O-i-Pr)$_6$, which can be crystallized from hexanes or pentanes as pale yellow platelike crystals (eq 3). (R$_2$BINO)Ti$_2$(O-i-Pr)$_6$

$$2\text{Ti}(O\text{-}i\text{-Pr})_4 + \text{H}_2\text{R}_2\text{BINO} \xrightarrow{-2i\text{-PrOH}}$$

$$\text{(R}_2\text{BINO)Ti}_2(O\text{-}i\text{-Pr})_6 \quad (3)$$

$$[\text{(R}_2\text{BINO)Ti}(O\text{-}i\text{-Pr})_2]_n + n\text{Ti}(O\text{-}i\text{-Pr})_4 \rightarrow$$

$$n\text{(R}_2\text{BINO)Ti}_2(O\text{-}i\text{-Pr})_6 \quad (4)$$

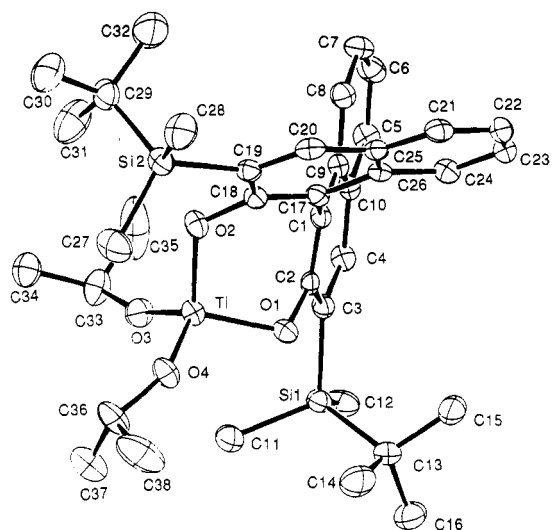complexes can also be prepared by mixing "(R$_2$BINO)-Ti(O-i-Pr)$_2$" derivatives with stoichiometric quantities of

(26) Bradley, D. C.; Mehrotra, R. C.; Wardlaw, W. *J. Chem. Soc.* **1952**, 5020.
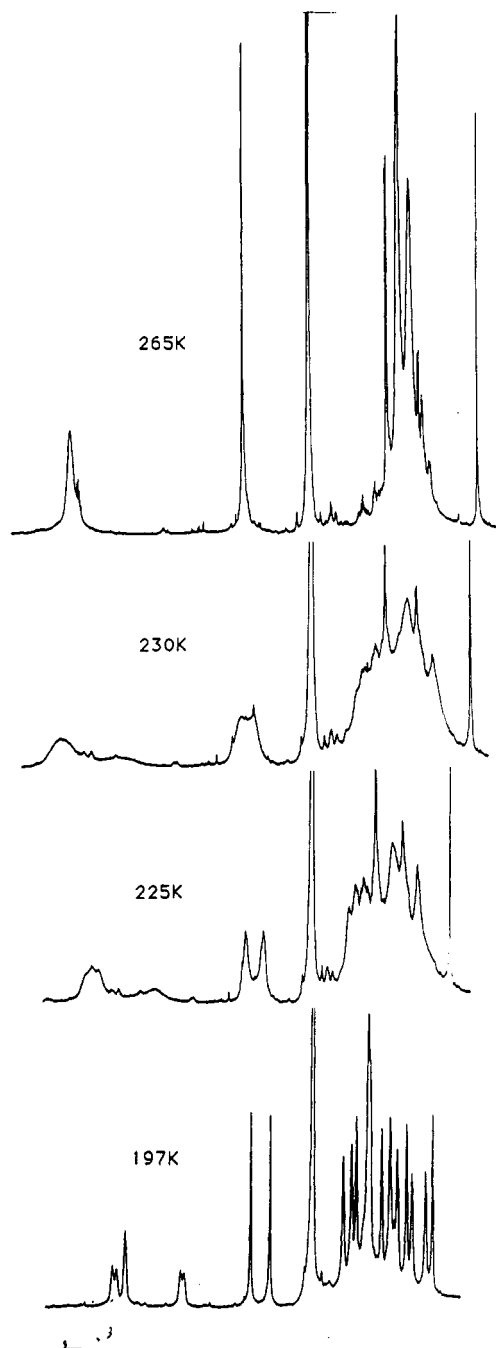
Figure 3. Variable-temperature 500-MHz ^{1}H NMR spectrum of (MeBINO)Ti$_2$(O-i-Pr)$_6$ (aliphatic region), showing the coalescence of the low-temperature C_1 structure to a time-averaged C_2-symmetric structure.

Figure 4. Molecular structure of {(t-BuMe$_2$Si)$_2$BINO}Ti(O-i-Pr)$_2$ with 50% probability thermal ellipsoids showing the atom-labeling scheme.

Ti(O-i-Pr)$_4$ (eq 4). A cryoscopic molecular weight determination demonstrated that (Me$_2$BINO)Ti$_2$(O-i-Pr)$_6$ exists as a dinuclear compound in solution. The reaction to form {(t-BuMe$_2$Si)$_2$BINO}Ti(O-i-Pr)$_2$ actually proceeds through a discrete {(t-BuMe$_2$Si)$_2$BINO}Ti$_2$(O-i-Pr)$_6$ intermediate (Scheme I), which is stable for days in the presence of excess H$_2$(t-BuMe$_2$Si)$_2$BINO. Refluxing in toluene promotes the rapid conversion of the intermediate complex to {(t-BuMe$_2$Si)$_2$BINO}Ti(O-i-Pr)$_2$.

The ^{1}H and ^{13}C NMR spectra of (Me$_2$BINO)Ti$_2$(O-i-Pr)$_6$, dissolved at 197 K in toluene-d_8 (see Figure 3 for the ^{1}H NMR spectrum),[27] are consistent with a fully static

(Me$_2$BINO)Ti$_2$(O-i-Pr)$_6$ skeleton having C_1 symmetry. Both of the naphtholate ring environments and all six diastereotopic i-PrO units are clearly visible at reduced temperature. As the temperature is increased toward 298 K, the disparate naphtholate and i-PrO environments undergo coalescence ($\Delta G^{\ddagger}_{240K}$ = 10.8 kcal/mol) to produce a time-averaged molecular structure with C_2 symmetry (Figure 3). Based on the demonstrated ability of the Me$_2$BINO ligand to act as a unidentate bridging ligand (vide infra) and the stability of 1,3-dioxadititanacycle units, we propose that the ground-state structure for this complex contains a Ti–O–Ti–O core, which could be bridged either by two i-PrO units or by both a naphtholate and an i-PrO ligand. Interestingly, spectra of the related {(t-BuMe$_2$Si)$_2$BINO}Ti$_2$(O-i-Pr)$_6$ derivative retain C_2 symmetry even at very low temperature (197 K), although a few resonances undergo slight broadening consistent with some differentiation of the i-PrO environments in a ground-state structure. The fast-exchange spectrum is similar to that of (Me$_2$BINO)Ti$_2$(O-i-Pr)$_6$, from which we infer that both of these (R$_2$BINO)Ti$_2$(O-i-Pr)$_6$ complexes have a common accessible bis-Ti(O-i-Pr)$_3$ substituted form.

Structural Studies of Titanium Binaphtholate Complexes. Molecular Structure of {(t-BuMe$_2$Si)$_2$BINO}Ti(O-i-Pr)$_2$. The molecular structure of {(t-BuMe$_2$Si)$_2$BINO}Ti(O-i-Pr)$_2$ is shown in Figure 4. Its positional and isotropic thermal parameters and a compilation of selected bond distances and angles are included in Tables I and II, respectively. The molecule is a mononuclear tetrahedral titanium (IV) complex, which displays a slight distortion from ideal T_d coordination due to the bidentate (t-BuMe$_2$Si)$_2$BINO ligand. The O$_{Ar}$(1)–Ti–O$_{Ar}$(2) angle is compressed to 104.3 (1)° to accommodate the binaphtholate chelate, while the O$_{Pr}$(3)–Ti–O$_{Pr}$(4) angle is splayed to 111.5 (1)° to relieve interactions between the remaining i-PrO ligands.

Consistent with comparisons between Ti–O$_{aromatic}$ and Ti–O$_{aliphatic}$ bond distances in analogous complexes, the Ti–O$_{Ar}$ distances are approximately 0.1 Å longer than the corresponding Ti–O$_{Pr}$ distances.[28,29] The shorter Ti–O$_{Pr}$

(27) For an example of the observation of kinetically trapped products by NMR spectroscopy, see: Bushweller, C. H.; Jenson, F. R. *J. Am. Chem. Soc.* **1968**, *90*, 2450.

(28) (a) Latesky, S. L.; Keddington, J.; McMullen, A. K.; Rothwell, I. P.; Huffman, J. C. *Inorg. Chem.* **1985**, *24*, 995. (b) Durfee, L. D.; Latesky, S. L.; Rothwell, I. P.; Huffman, J. C.; Folting, K. *Inorg. Chem.* **1985**, *24*, 4569.
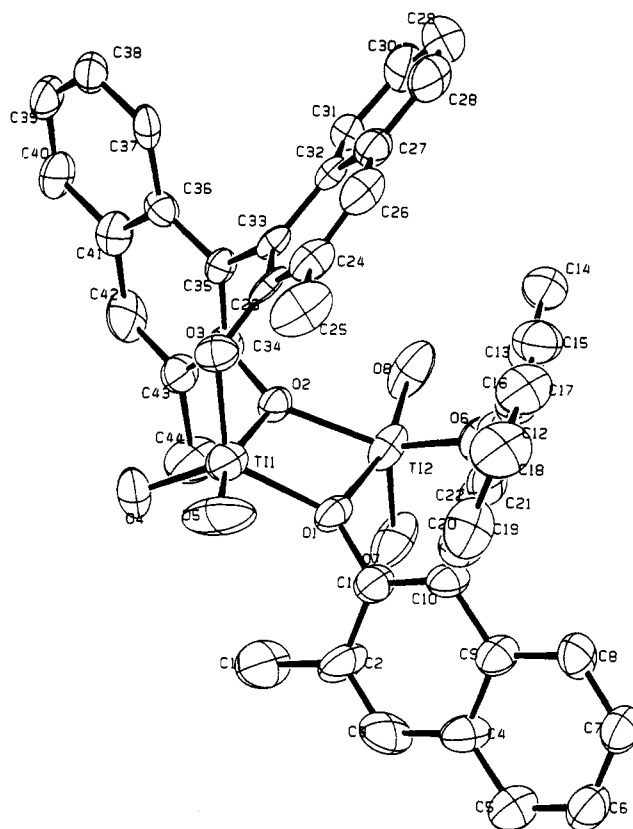
Table I. Positional and Isotropic Thermal Parameters for
{(t-BuMe₂Si)₂BINO}Ti(O-i-Pr)₂

atom	x	y	z	B(eq), Å²
Ti(1)	0.94101 (4)	0.16722 (3)	0.24608 (2)	1.76 (3)
Si(1)	1.24653 (7)	0.13797 (5)	0.38942 (3)	1.92 (4)
Si(2)	0.78318 (7)	0.25410 (5)	0.06229 (3)	2.17 (4)
O(1)	1.0868 (2)	0.2202 (1)	0.28024 (7)	1.85 (8)
O(2)	0.9481 (2)	0.1707 (1)	0.16664 (8)	2.02 (8)
O(3)	0.9371 (2)	0.0599 (1)	0.26659 (8)	2.50 (9)
O(4)	0.8133 (2)	0.2265 (1)	0.26434 (8)	2.51 (9)
C(1)	1.2104 (2)	0.1841 (2)	0.2068 (1)	1.5 (1)
C(2)	1.1886 (2)	0.1792 (2)	0.2642 (1)	1.5 (1)
C(3)	1.2665 (2)	0.1330 (2)	0.3092 (1)	1.7 (1)
C(4)	1.3626 (3)	0.0874 (2)	0.2919 (1)	1.9 (1)
C(5)	1.4806 (3)	0.0318 (2)	0.2163 (1)	2.1 (1)
C(6)	1.4993 (3)	0.0279 (2)	0.1596 (1)	2.4 (1)
C(7)	1.4224 (3)	0.0742 (2)	0.1168 (1)	2.3 (1)
C(8)	1.3288 (3)	0.1252 (2)	0.1310 (1)	2.1 (1)
C(9)	1.3082 (2)	0.1320 (2)	0.1898 (1)	1.7 (1)
C(10)	1.3845 (2)	0.0831 (2)	0.2332 (1)	1.7 (1)
C(11)	1.0938 (2)	0.0948 (3)	0.4030 (2)	3.0 (2)
C(12)	1.3712 (3)	0.0681 (2)	0.4288 (2)	3.0 (2)
C(13)	1.2706 (3)	0.2517 (2)	0.4192 (1)	2.3 (1)
C(14)	1.1478 (4)	0.3022 (3)	0.4109 (2)	3.6 (2)
C(15)	1.3653 (3)	0.2984 (2)	0.3884 (1)	3.0 (2)
C(16)	1.3206 (4)	0.2476 (3)	0.4849 (1)	3.4 (2)
C(17)	1.1399 (2)	0.2433 (2)	0.1630 (1)	1.7 (1)
C(18)	1.0144 (2)	0.2331 (2)	0.1427 (1)	1.7 (1)
C(19)	0.9477 (2)	0.2824 (2)	0.0962 (1)	1.8 (1)
C(20)	1.0113 (3)	0.3488 (2)	0.0753 (1)	1.9 (1)
C(21)	1.1980 (3)	0.4387 (2)	0.0761 (1)	2.1 (1)
C(22)	1.3206 (3)	0.4551 (2)	0.0954 (1)	2.3 (1)
C(23)	1.3870 (3)	0.4007 (2)	0.1373 (1)	2.2 (1)
C(24)	1.3309 (3)	0.3321 (2)	0.1594 (1)	2.0 (1)
C(25)	1.1371 (3)	0.3679 (2)	0.0966 (1)	1.7 (1)
C(26)	1.2036 (2)	0.3133 (2)	0.1399 (1)	1.7 (1)
C(27)	0.6740 (3)	0.2550 (3)	0.1171 (2)	3.5 (2)
C(28)	0.7325 (4)	0.3416 (2)	0.0080 (2)	3.4 (2)
C(29)	0.7790 (3)	0.1475 (2)	0.0219 (1)	2.6 (1)
C(30)	0.6548 (4)	0.1424 (3)	−0.0201 (2)	4.4 (2)
C(31)	0.7857 (5)	0.0705 (3)	0.0626 (2)	4.8 (2)
C(32)	0.8844 (4)	0.1442 (3)	−0.0145 (2)	4.9 (2)
C(33)	0.9451 (3)	−0.0324 (2)	0.2634 (2)	2.8 (1)
C(34)	0.8253 (3)	−0.0655 (2)	0.2309 (2)	3.1 (2)
C(35)	1.0553 (4)	−0.0544 (3)	0.2345 (4)	7.2 (3)
C(36)	0.6924 (3)	0.2272 (2)	0.2820 (2)	3.2 (2)
C(37)	0.6948 (4)	0.1721 (3)	0.3352 (2)	3.9 (2)
C(38)	0.6533 (5)	0.3169 (3)	0.2894 (2)	5.2 (2)

Table II. Selected Intramolecular Bond Distances (Å) and
Angles (deg) for {(t-BuMe₂Si)₂BINO}Ti(O-i-Pr)₂

Distances

Ti(1)–O(1)	1.852 (2)	O(1)–C(2)	1.376 (3)
Ti(1)–O(2)	1.846 (2)	O(2)–C(18)	1.374 (3)
Ti(1)–O(3)	1.740 (2)	O(3)–C(33)	1.441 (4)
Ti(1)–O(4)	1.769 (2)	O(4)–C(36)	1.434 (4)
Si(1)–C(3)	1.897 (3)		
Si(2)–C(19)	1.891 (3)		

Angles

O(1)–Ti(1)–O(2)	104.28 (8)	Ti(1)–O(1)–C(2)	110.4 (1)
O(1)–Ti(1)–O(3)	111.54 (9)	Ti(1)–O(2)–C(18)	121.5 (2)
O(1)–Ti(1)–O(4)	108.48 (9)	Ti(1)–O(3)–C(33)	160.0 (2)
		Ti(1)–O(4)–C(36)	149.0 (2)

bonds reflect the higher basicity and π-bonding capacity of the aliphatic alkoxide ligands.[28] It is noteworthy that the 1.85-Å (av) Ti–O$_{Ar}$ bonds are among the longest observed in four-coordinate Ti complexes. Moreover, the 115° (av) Ti–O–C$_{Ar}$ angles are unusually small by comparison with M–O–C$_{Ar}$ angles of 150–159° typically found for highly sterically demanding 2,6-disubstituted phen-

(29) (a) Olmskao, M. M.; Sigel, G.; Hope, H.; Xu, X.; Power, P. R. *J. Am. Chem. Soc.* **1985**, *107*, 3087. (b) Bott, S. G.; Coleson, A. W.; Atwood, J. L. *J. Chem. Soc., Chem. Commun.* **1986**, 610. (c) Dilworth, J. L.; Hanich, J.; Beck, J.; Straehle, J. *J. Organomet. Chem.* **1986**, *315*, C9.

Figure 5. Molecular structure of [(Me₂BINO)Ti(O-i-Pr)₂]₂ with 50% probability thermal ellipsoids showing the atom-labeling scheme. The carbon atoms of the isopropoxide ligands are omitted for clarity.

oxide ligands.[28] We hypothesize that the observed angles are adopted primarily to allow the binaphtholate ligand to accommodate the 2.9–3.0-Å O···O distance typical of a four-coordinate Ti complex.[28,29] This relatively fixed bite distance and the binaphthyl ring junction impose a restriction on the Ti–O–C$_{Ar}$ angle. This effect would enforce an even more acute angle were the titanium center in an ideal T_d coordination environment. The small Ti–O–C$_{Ar}$ angle may also limit the ability of the ligand to engage in π-bonding and could contribute to the noteworthy length of the Ti–O$_{Ar}$ bonds. The angular constraints imposed on the (t-BuMe₂Si)₂BINO ligand in this molecule are in sharp constrast to the evident flexibility of i-PrO bonding. Although the angular extension observed for Ti–O(3)–C(33) and Ti–O(4)–C(36) (160.0 (3)° and 149.0 (2)°, respectively) might be attributed to a simple geometrical distortion to reduce interligand interactions, the relatively short Ti–O$_{Pr}$ distances provide further evidence that these bonds possess a significant degree of Ti–O π-bond character. The silyl substituents adopt conformations that place the t-Bu groups adjacent to the exo faces of the naphthalene rings. Peri interactions between the Si and O substituents are sufficient to extend the dihedral angle between the C$_{Ar}$–O and C$_{Ar}$–Si bonds to 7.9 (3)°, with the silyl substituent being shifted toward the exo face of the naphthalene ring.

Molecular Structure of (R*,R*)-[(Me₂BINO)Ti(O-i-Pr)₂]₂. A view of the molecular structure of [(Me₂BINO)Ti(O-i-Pr)₂]₂ oblique to the 1,3-dioxaditanacycle is shown in Figure 5. Positional and isotropic thermal parameters, and selected bond distances and angles are collected in Tables III and IV, respectively. The X-ray crystallographic study confirms the structure deduced from NMR spectroscopy. The molecule exists as a dimer having virtual C_2 symmetry, in which the 1,3-di-

Table III. Positional and Isotropic Thermal Parameters for [(Me₂BINO)Ti(O-*i*-Pr)₂]₂

atom	x	y	z	B(eq), Å²	atom	x	y	z	B(eq), Å²
Ti(1)	0.8427 (1)	0.2270 (2)	0.86292 (8)	3.8 (1)	C(24)	0.6585 (7)	0.419 (1)	0.8338 (4)	3.6 (6)
Ti(2)	0.7367 (1)	0.0098 (2)	0.90408 (8)	3.6 (1)	C(25)	0.682 (1)	0.440 (1)	0.7822 (5)	5.8 (8)
O(1)	0.7982 (4)	0.0672 (6)	0.8463 (3)	3.2 (3)	C(26)	0.5852 (7)	0.437 (1)	0.8413 (4)	3.9 (6)
O(2)	0.7925 (3)	0.1610 (6)	0.9250 (2)	2.6 (3)	C(27)	0.5637 (6)	0.416 (1)	0.8888 (5)	3.3 (6)
O(3)	0.7872 (4)	0.3634 (6)	0.8691 (3)	3.3 (4)	C(28)	0.4871 (7)	0.428 (1)	0.8958 (5)	4.9 (7)
O(4)	0.9338 (4)	0.2355 (8)	0.9045 (3)	5.7 (5)	C(29)	0.4657 (7)	0.400 (1)	0.9413 (6)	5.2 (8)
O(5)	0.8661 (5)	0.2495 (8)	0.8021 (4)	7.3 (5)	C(30)	0.5201 (8)	0.356 (1)	0.9823 (5)	4.2 (7)
O(6)	0.6555 (4)	−0.0129 (7)	0.8502 (3)	3.8 (4)	C(31)	0.5956 (6)	0.344 (1)	0.9781 (4)	3.0 (5)
O(7)	0.7901 (5)	−0.1255 (7)	0.9142 (3)	5.3 (4)	C(32)	0.6196 (6)	0.3738 (9)	0.9318 (4)	2.5 (5)
O(8)	0.6879 (5)	0.0090 (7)	0.9567 (3)	5.3 (4)	C(33)	0.6974 (6)	0.3612 (9)	0.9259 (4)	2.4 (5)
C(1)	0.8036 (6)	−0.015 (1)	0.8083 (4)	3.7 (6)	C(34)	0.8021 (6)	0.228 (1)	0.9694 (4)	2.7 (5)
C(2)	0.8730 (7)	−0.083 (1)	0.8141 (5)	4.7 (7)	C(35)	0.7586 (6)	0.329 (1)	0.9707 (4)	2.1 (5)
C(3)	0.8781 (7)	−0.174 (1)	0.7806 (5)	4.8 (7)	C(36)	0.7748 (5)	0.405 (1)	1.0162 (4)	2.5 (5)
C(4)	0.8145 (7)	−0.210 (1)	0.7410 (5)	4.1 (6)	C(37)	0.7374 (6)	0.516 (1)	1.0204 (4)	3.0 (5)
C(5)	0.8181 (8)	−0.309 (1)	0.7063 (5)	4.5 (7)	C(38)	0.7533 (6)	0.585 (1)	1.0642 (5)	3.4 (6)
C(6)	0.7593 (8)	−0.340 (1)	0.6698 (5)	4.4 (7)	C(39)	0.8084 (7)	0.548 (1)	1.1067 (5)	3.9 (6)
C(7)	0.6891 (7)	−0.275 (1)	0.6651 (5)	4.6 (7)	C(40)	0.8468 (6)	0.444 (1)	1.1041 (4)	3.9 (6)
C(8)	0.6818 (7)	−0.179 (1)	0.6978 (4)	4.0 (6)	C(41)	0.8325 (6)	0.368 (1)	1.0586 (4)	3.3 (6)
C(9)	0.7444 (7)	−0.142 (1)	0.7356 (4)	3.6 (6)	C(42)	0.8724 (6)	0.259 (1)	1.0549 (4)	4.2 (6)
C(10)	0.7413 (6)	−0.041 (1)	0.7700 (4)	3.1 (5)	C(43)	0.8601 (6)	0.189 (1)	1.0116 (4)	3.1 (5)
C(11)	0.9390 (8)	−0.055 (2)	0.8588 (6)	6.4 (7)	C(44)	0.9021 (9)	0.073 (1)	1.0079 (6)	5.3 (7)
C(12)	0.6304 (7)	0.042 (1)	0.8049 (5)	3.8 (6)	C(45)	1.001 (1)	0.305 (2)	0.9155 (8)	8 (1)
C(13)	0.5606 (7)	0.110 (1)	0.8000 (5)	4.4 (7)	C(46)	1.063 (1)	0.227 93)	0.937 (1)	17 (2)
C(14)	0.5206 (9)	0.111 (1)	0.8447 (6)	5.5 (8)	C(47)	0.991 (1)	0.407 (2)	0.947 (1)	15 (2)
C(15)	0.5350 (8)	0.174 (1)	0.7550 (6)	4.9 (7)	C(48)	0.875 (1)	0.260 (3)	0.747 (1)	14 (2)
C(16)	0.5750 (7)	0.174 (1)	0.7140 (5)	4.2 (6)	C(49)	0.936 (1)	0.181 (3)	0.743 (1)	16 (2)
C(17)	0.5502 (8)	0.245 (1)	0.6679 (5)	5.2 (7)	C(50)	0.906 (2)	0.386 (3)	0.748 (2)	31 (4)
C(18)	0.5930 (9)	0.249 (1)	0.6283 (6)	6.4 (8)	C(51)	0.776 (1)	−0.252 (1)	0.9257 (6)	7.3 (9)
C(19)	0.6625 (9)	0.183 (1)	0.6325 (5)	5.7 (7)	C(52)	0.842 (1)	−0.325 (1)	0.9143 (6)	9 (1)
C(20)	0.6868 (8)	0.112 (1)	0.6765 (5)	4.5 (7)	C(53)	0.697 (1)	−0.287 (1)	0.8924 (6)	8.4 (9)
C(21)	0.6434 (7)	0.105 (1)	0.7186 (4)	3.7 (6)	C(54)	0.6429 (9)	0.014 (1)	0.9969 (5)	6.4 (8)
C(22)	0.6700 (6)	0.036 (1)	0.7650 (4)	3.3 (6)	C(55)	0.695 (1)	0.019 (2)	1.0476 (5)	10 (1)
C(23)	0.7153 (7)	0.3788 (9)	0.8779 (4)	3.0 (6)	C(56)	0.598 (1)	−0.106 (2)	0.9895 (7)	15 (2)

Table IV. Selected Intramolecular Bond Distances (Å) and Angles (deg) for [(Me₂BINO)Ti(O-*i*-Pr)₂]₂

Distances

Ti(1)–O(1)	1.953 (7)	O(1)–C(1)	1.37 (1)
Ti(1)–O(2)	2.128 (7)	O(2)–C(34)	1.36 (1)
Ti(1)–O(3)	1.827 (7)	O(3)–C(23)	1.35 (1)
Ti(1)–O(4)	1.771 (8)	O(4)–C(45)	1.41 (2)
Ti(1)–O(5)	1.741 (9)	O(5)–C(48)	1.48 (2)
Ti(2)–O(1)	2.127 (7)	Ti(1)–Ti(2)	3.297 (1)

Angles

O(1)–Ti(1)–O(2)	69.5 (2)	O(3)–Ti(1)–O(5)	100.9 (4)
O(1)–Ti(1)–O(3)	124.6 (3)	O(4)–Ti(1)–O(5)	102.0 (5)
O(1)–Ti(1)–O(4)	117.9 (3)	Ti(1)–O(1)–Ti(2)	110.6 (3)
O(1)–Ti(1)–O(5)	94.7 (3)	Ti(1)–O(2)–Ti(2)	109.9 (3)
O(3)–Ti(1)–O(4)	110.2 (4)		

oxadititanacycle is supported by two bridging naphtholate units (one from each of the two Me₂BINO ligands). The coordination environment about each Ti center is best described as a highly distorted trigonal bipyramid, with a bridging naphtholate ligand and one *i*-PrO ligand occupying the axial positions (i.e., O(2) and O(5) with respect to Ti(1)), and one *i*-PrO, a terminal naphtholate and a bridging naphtholate ligand occupying the remaining equatorial sites (i.e., O(4), O(3), and O(1), respectively, with respect to Ti(1)). As we inferred from NMR studies, the absolute configurations of the two binaphtholate units within a single molecule are identical.

Individual titanium–oxygen interactions in [(Me₂BINO)Ti(O-*i*-Pr)₂]₂ are quite similar to those observed in {(*t*-BuMe₂Si)₂BINO}Ti(O-*i*-Pr)₂. Ti–O$_{Pr}$ distances are nearly 0.1 Å shorter than Ti–O$_{Ar}$ distances. As is typically observed in ligands adopting a bridging position, the Ti–μ-O$_{Ar}$ distances are a minimum of 0.1 Å longer than terminal Ti–O$_{Ar}$ bonds. The central Ti(1)–O(1)–Ti(2)–O(2) core shows a significant variation in the Ti–O bond distances, with an axial Ti(1)–O(2) bond length of 2.128 (7) Å and an equatorial Ti(2)–O(2) bond length of 1.970 (7)

Å. These variations in Ti–μ-O$_{Ar}$ distances indicate that the Ti–μ-O$_{Ar}$ bonds between the two (Me₂BINO)Ti(O-*i*-Pr)₂ fragments are significantly more stable than the Ti–μ-O$_{Ar}$ bonds that produce the chelate. An increased axial Ti–μ-O$_{Ar}$ distance is expected, because axial bridging ligands generally engender more severe steric interactions and experience greater competition for empty dπ-bonding orbitals than analogous equatorial ligands.[30] The axial *i*-PrO ligand clearly does not suffer in its ability to π-bond as is evidenced by the nearly insignificant difference between axial and equatorial Ti–O$_{Pr}$ distances (ΔTi–O$_{Pr}$ = 0.030 Å). The axial *i*-PrO ligand evidently gains π-bonding capacity at the expense of the *trans*-μ-naphthoxide ligand.

The 1,3-dioxadititanacycle core shows a slight (6.7 (2)°) puckering, which is more clearly visible in a view of the molecule down the Ti(1)⋯Ti(2) axis (Figure 6). The Ti(1)⋯Ti(2) distance of 3.30 Å and the internal angles of the 1,3-dioxadititanacycle are consistent with distances and angles observed in other d⁰-d⁰ dinuclear complexes containing a Ti–O–Ti–O core.[32,33] The major distortions from ideal trigonal-bipyramidal geometry about each titanium center are the reduction of the μ-O$_{ax}$–Ti–μ-O$_{eq}$ angle from an idealized 90° to 69.4° (av) and the reduction of the O$_{ax}$–Ti–μ-O$_{ax}$ angle from 180° to 163.0° (av). Nearly

(30) Chisholm, M. H.; Huffman, J. C.; Marchant, N. S. *J. Am. Chem. Soc.* **1983**, *105*, 6162.

(31) (a) Watenpaugh, K.; Caughlan, C. N. *Inorg. Chem.* **1966**, *5*, 1782. (b) Stoeckli-Evans, H. *Helv. Chim. Acta* **1975**, *58*, 373.

(32) Other doubly bridged dimer structures involving Ti include references in this citation and in ref 33. (a) Borgias, B. A.; Cooper, S. R.; Koh, Y. B.; Raymond, K. N. *Inorg. Chem.* **1984**, *23*, 1009. (b) Harlow, R. L. *Acta Crystallogr.* **1983**, *39*, 1344. (c) Svetich, G. W.; Voge, A. A. *Acta Crystallogr.* **1972**, *B28*, 1760. (d) Smith, G. D.; Caughlin, C. N.; Campbell, J. A. *Inorg. Chem.* **1972**, *11*, 2989.

(33) (a) Sharpless, K. B. *Chem. Scr.* **1987**, *27*, 521. (b) Sharpless, K. B.; Pedersen, S. F.; Dewan, J. C.; Eckman, R. R. *J. Am. Chem. Soc.* **1987**, *109*, 1279. (c) Williams, I. D.; Pedersen, S. F.; Sharpless, K. B.; Lippard, S. J. *J. Am. Chem. Soc.* **1984**, *106*, 6430.
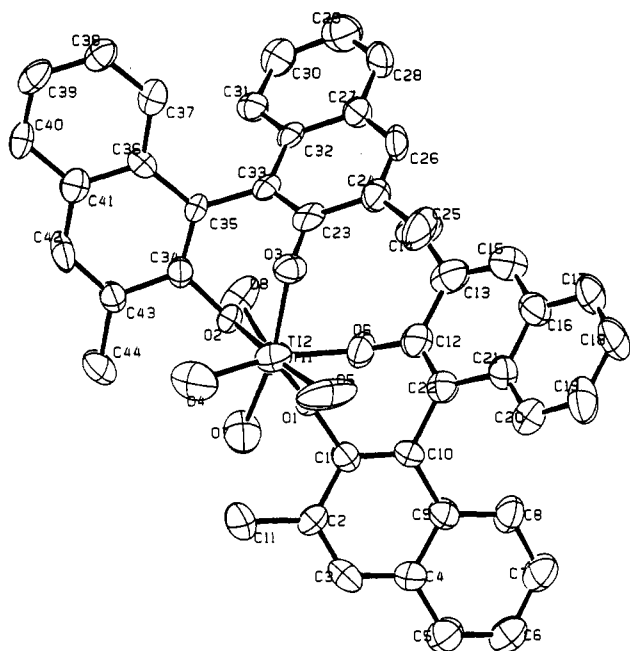
Figure 6. View of [(Me₂BINO)Ti(O-*i*-Pr)₂]₂ down the Ti(1)⋯Ti(2) axis.

identical angular characteristics are observed in every known edge-fused bis-trigonal-bipyramidal titanium dimer.[31-33] The tied-back O–Ti–O–Ti ring evidently allows the O_{ax} ligand to cant toward the μ-O_{eq} ligand. Consistent with this explanation, the reduction in the O_{ax}-Ti-μ-O_{ax} angle observed in [(Me₂BINO)Ti(O-*i*-Pr)₂]₂ and every known complex of this type occurs through the bending of the O_{ax} ligand toward the μ-O_{eq} ligand.[31]

The pairing of binaphtholate ligands of like chirality in (*R**,*R**)-[(Me₂BINO)Ti(O-*i*-Pr)₂]₂ results in striking differentiation of the faces of the 1,3-dioxadititanacycle unit (Figure 6). The slight puckering of the 1,3-Ti₂O₂ ring, noted previously, probably arises from the efforts of the terminal *syn*-naphtholate groups to avoid steric contact. In fact, two other characteristics of Me₂BINO ligand bonding help to reduce unfavorable intramolecular interactions in the dimer. First, the terminal naphtholate expands its Ti–O–C$_{Ar}$ bond angle to 133° (av) to reduce contact between the *syn*-naphtholate moieties. Second, the (*R*)-Me₂BINO ligand (take, for example, the (*R*)-Me₂BINO ligand characterized by O(2) and O(3) in Figure 6) adopts a λ rather than a δ bridging mode. The same ligand could adopt a δ bridging environment by forming its terminal attachment at the diastereotopic O(4) bridging site. Based on simple model structures, this alternative ligand orientation would engender intraligand strain by dramatically reducing the dihedral angle between the naphthalene rings. Moreover, the δ configuration would cause the naphtholate unit bonded to O(2) to rotate into the plane of the 1,3-dioxadititanacycle, generating a destabilizing contact between the C(44) methyl substituent and the O(8) isopropoxide group.

Molecular Structure of {(*t*-BuMe₂Si)₂BINO}Ti₂(O-*i*-Pr)₆. A view of the molecular structure of {(*t*-BuMe₂Si)₂BINO}Ti₂(O-*i*-Pr)₆ perpendicular to the naphtholate ring junction is shown in Figure 7. Positional and isotropic thermal parameters, together with selected bond distances and angles, are collected in Tables V and VI, respectively. Characteristics such as the Ti–O bond distances, the exo orientation of the *t*-Bu unit, and slight distortions from planarity due to Si–O peri interactions are similar to those observed in previous R₂BINO com-

Table V. Positional and Isotropic Thermal Parameters for {(*t*-BuMe₂Si)₂BINO}Ti₂(O-*i*-Pr)₆

| atom	x	y	z	B(eq), Å²
Ti(1)	0.15487 (6)	0.17792 (5)	0.68032 (4)	2.98 (4)
Si(1)	0.25783 (8)	0.13774 (7)	0.88671 (6)	2.46 (6)
O(1)	0.1339 (2)	0.1409 (1)	0.7593 (1)	2.2 (1)
O(2)	0.0613 (3)	0.2278 (4)	0.6493 (3)	10.0 (4)
O(3)	0.2496 (3)	0.2365 (2)	0.6921 (2)	5.5 (2)
O(4)	0.1815 (4)	0.1124 (2)	0.6257 (2)	7.2 (3)
C(1)	0.0216 (3)	0.0540 (2)	0.7836 (2)	1.6 (2)
C(2)	0.0982 (3)	0.0942 (2)	0.8017 (2)	1.7 (2)
C(3)	0.1458 (3)	0.0887 (2)	0.8638 (2)	1.7 (2)
C(4)	0.1122 (3)	0.0409 (2)	0.9062 (2)	1.9 (2)
C(5)	0.0033 (3)	-0.0556 (2)	0.9333 (2)	2.2 (2)
C(6)	-0.0703 (3)	-0.0983 (3)	0.9164 (2)	2.8 (2)
C(7)	-0.1162 (3)	-0.0908 (3)	0.8563 (2)	2.7 (2)
C(8)	-0.0884 (3)	-0.0417 (2)	0.8129 (2)	2.2 (2)
C(9)	-0.0115 (3)	0.0034 (2)	0.8287 (2)	1.7 (2)
C(10)	0.0342 (3)	-0.0036 (2)	0.8904 (2)	1.9 (2)
C(11)	0.2629 (5)	0.2315 (3)	0.8585 (3)	3.5 (3)
C(12)	0.2711 (5)	0.1411 (5)	0.9768 (3)	4.5 (3)
C(13)	0.3583 (3)	0.0856 (3)	0.8561 (3)	3.8 (2)
C(14)	0.3428 (5)	0.0687 (4)	0.7843 (3)	5.0 (3)
C(15)	0.4472 (4)	0.1313 (5)	0.8658 (5)	7.0 (4)
C(16)	0.3718 (6)	0.0166 (4)	0.8949 (5)	6.3 (4)
C(17)	-0.0078 (5)	0.2620 (4)	0.6124 (5)	7.8 (5)
C(18)	-0.0288 (8)	0.3338 (5)	0.6396 (8)	13.8 (9)
C(19A)	0.044 (1)	0.286 (2)	0.547 (1)	15.9
C(19B)	-0.005 (2)	0.233 (1)	0.549 (1)	11.1
C(20)	0.3120 (6)	0.2915 (4)	0.6754 (5)	8.0 (5)
C(21)	0.2692 (6)	0.3616 (4)	0.6772 (4)	7.6 (5)
C(22A)	0.4072 (9)	0.2837 (8)	0.704 (1)	6.7
C(22B)	0.375 (1)	0.2680 (8)	0.637 (1)	8.6
C(23)	0.2229 (5)	0.0709 (4)	0.5779 (3)	5.9 (3)
C(24)	0.2378 (7)	0.1222 (5)	0.5208 (4)	9.6 (5)
C(25)	0.3058 (5)	0.0324 (6)	0.6068 (4)	9.1 (5)
H(4)	0.140 (3)	0.035 (2)	0.944 (2)	1.5 (8)
H(5)	0.038 (3)	-0.057 (2)	0.974 (2)	1.4 (8)
H(6)	-0.092 (3)	-0.133 (2)	0.941 (2)	1.8 (9)
H(7)	-0.161 (3)	-0.111 (2)	0.849 (2)	2 (1)
H(8)	-0.121 (2)	-0.038 (2)	0.774 (2)	0.3 (7)
H(11A)	0.320 (5)	0.249 (3)	0.872 (3)	6 (2)
H(11B)	0.276 (4)	0.225 (3)	0.805 (3)	6 (2)
H(11C)	0.230 (5)	0.256 93)	0.873 (4)	6 (2)
H(12A)	0.291 (4)	0.090 (4)	0.991 (3)	6 (2)
H(12B)	0.335 (5)	0.158 (3)	0.986 (3)	6 (1)
H(12C)	0.235 (5)	0.169 (4)	0.989 (3)	6 (2)
H(14A)	0.276 (6)	0.042 (4)	0.769 (4)	10 (2)
H(14B)	0.334 (5)	0.116 (4)	0.759 (4)	8 (2)
H(14C)	0.390 (5)	0.042 (3)	0.761 (3)	6 (2)
H(15A)	0.4989	0.1049	0.8511	12 (3)
H(15B)	0.4405	0.1744	0.8420	16 (5)
H(15C)	0.452 (5)	0.136 (4)	0.923 (4)	8 (2)
H(16A)	0.306 (5)	-0.011 (4)	0.885 (3)	7 (2)
H(16B)	0.419 (6)	-0.010 (4)	0.893 (4)	9 (2)
H(16C)	0.3856	0.0276	0.9401	16 (4)
H(23)	0.1755	0.0339	0.5614	8 (2)
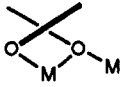
Table VI. Intramolecular Distances (Å) and Angles (deg) for {(*t*-BuMe₂Si)₂BINO}Ti₂(O-*i*-Pr)₆

Distances			
Ti(1)–O(1)	1.825 (3)	Ti(1)–O(3)	1.756 (4)
Ti(1)–O(2)	1.731 (5)	Ti(1)–O(4)	1.730 (4)

Angles			
O(1)–Ti(1)–O(2)	111.6 (2)	Ti(1)–O(1)–C(2)	156.2 (3)
O(1)–Ti(1)–O(3)	106.5 (2)	Ti(1)–O(2)–C(17)	168.0 (7)
O(1)–Ti(1)–O(4)	112.3 (2)	Ti(1)–O(3)–C(20)	156.1 (5)
O(2)–Ti(1)–O(3)	107.4 (3)	Ti(1)–O(4)–C(23)	164.9 (4)
O(2)–Ti(1)–O(4)	109.8 (3)		
O(3)–Ti(1)–O(4)	109.1 (2)		

plexes of titanium (vide infra). The torsional angle subtended by the (*t*-BuMe₂Si)₂BINO ligands is strongly reminiscent of the bridging Me₂BINO ligand in (Me₂BINO)W₂(O-*t*-Bu)₄.[23a] This angle places the O(2)⋯O(2′) distance in excess of 3.5 Å and evidently relieves steric contact between the Ti(O-*i*-Pr)₃ unit and the silyl

Table VII. Summary of Structural Characteristics for Binaphtholate Complexes

	chelating	unidentate bridging	bidentate	unidentate
D(M–M), Å		3.2	2.35	4.2
dihedral angle, deg	66–68	62	90	89
D(M–O$_{Ar}$), Å	1.849 (Ti)	1.835 (1.964, 2.124) (Ti)	1.917 (W)	1.825 (Ti)
D(M–O$_{Al}$), Å	1.756 (Ti)	1.750 (Ti)	1.873 (W)	1.73, 1.735 (Ti)
M–O$_{Ar}$–C, deg	116.0	130.0	127.7	156.1
M–O$_{Al}$–C, deg	155.0	156.4	138.2	156.1, 164.9, 168.0
ligand	(t-BuMe$_2$Si)$_2$BINO	Me$_2$BINO	Me$_2$BINO	(t-BuMe$_2$Si)$_2$BINO
coordn no.	4 and 5	5	4	4
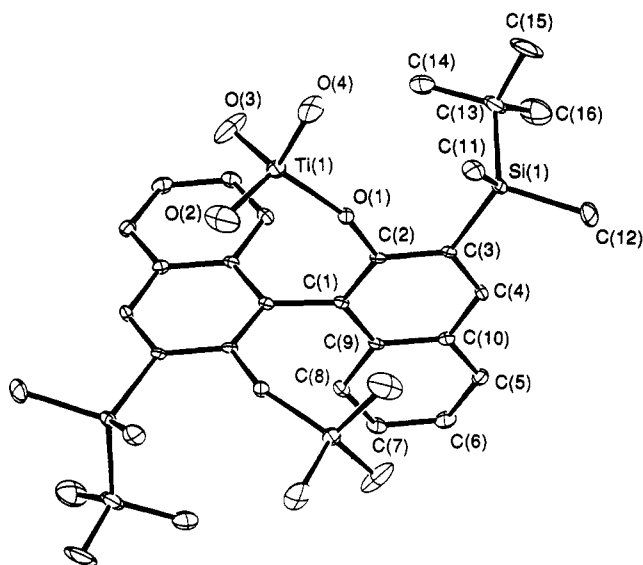
Figure 7. Molecular structure of {(t-BuMe$_2$Si)$_2$BINO}Ti$_2$(O-i-Pr)$_6$ with 50% probability thermal ellipsoids showing the atom-labeling scheme. The i-Pr units have been omitted for clarity. Note that the molecular structure is constrained by a crystallographic C$_2$-symmetry axis.

substituent on the opposing naphtholate ring (e.g., Ti(1) and Si(1′)). Attempts to close the distance between the two Ti centers to allow formation of a 1,3-dioxodititanacycle by either decreasing the dihedral angle of the naphtholate or by rotating the Ti(O-i-Pr)$_3$ units toward one another would, necessarily, increase these steric interactions.

This structure is quite reminiscent of the bis-TiCl$_3$L complex of trans-1,2-cyclohexanediol recently reported by Wuest.[34] In this latter system, the bite distance imposed by the cyclohexane unit was evidently sufficient to prevent the cyclohexanediol from acting as a unidentate bridging ligand. Despite this restriction, the halide complex achieves octahedral coordination by ligating two solvent molecules and establishing chloride bridges. The evident lack of steric demands in both the chloride and adjacent diolate ligand evidently facilitates this more condensed structure.

Analysis of Binaphtholate Coordination Chemistry. The structures of [(Me$_2$BINO)Ti(O-i-Pr)$_2$]$_2$, which contains a unidentate bridging Me$_2$BINO ligand, and {(t-BuMe$_2$Si)$_2$BINO}Ti$_2$(O-i-Pr)$_6$, which contains a bridging (t-BuMe$_2$Si)$_2$BINO unit, add two additional bonding modes to the known coordination chemistry of the binaphtholate ligand. Complexes containing a chelating

binaphtholate unit, similar to that observed in {(t-BuMe$_2$Si)$_2$BINO}Ti(O-i-Pr)$_2$, were first structured in 1980 by Brintzinger.[35] We previously identified the first bridging binaphtholate ligand spanning the 2.35-Å W≡W bond in (Me$_2$BINO)W$_2$(O-t-Bu)$_4$.[23a] The chelating binaphtholate bridge in [(Me$_2$BINO)Ti(O-i-Pr)$_2$]$_2$, while representing the first published example of this bonding mode for the R$_2$BINO ligand, is common among other diolate units. For example, Sharpless and Pedersen have shown that tartrate ligands in a variety of group 4 complexes habitually adopt this bonding mode.[33]

A summary of characteristic distances and angles associated with the four known R$_2$BINO ligating modes is shown in Table VII. The data demonstrate that binaphtholate ligands are capable of spanning a wide range of O···O distances, from 2.67 to 3.66 Å. During this increase in bite distance, the dihedral angle between the naphtholate units increases from 62° to 90°. Typical dihedral angles for chelating ligands containing either binaphtholate or BINAP (2,2′-bis(diphenylphosphino)-1,1′-binaphthyl) ligands vary between 67° and 70°.[35,36] Obviously, the binaphtholate ligand has the flexibility to accommodate a significant range of binding modes and coordination environments.

The observed conformations of the seven- and eight-membered rings formed by the R$_2$BINO ligands bear little resemblance to those found for cyclooctane and cycloheptane. This is hardly surprising, as the extended bond distances and expanded internal angles associated with an oxygen or titanium center, together with the angular restrictions imposed by the fused arene framework, should have a dramatic influence on the relative stability of various conformers. A notable characteristic of the Me$_2$BINO ligands in both (Me$_2$BINO)W$_2$(O-t-Bu)$_4$ and [(Me$_2$BINO)Ti(O-i-Pr)$_2$]$_2$ is that ligands having an R absolute configuration tend to form bridges having a λ arrangement with respect to the M···M vector.[23a] As we noted in the previous section, there are several potential reasons for the greater stability of this diastereomeric linkage. Some of these reasons, such as intramolecular ligand–ligand interactions, are molecule-specific and would not require that a R$_λ$ conformation have consistently greater stability. In contrast, model studies indicate that a decrease in the dihedral angle between the naphthalene rings, which invariably accompanies a change from a λ to a δ configuration in (R)-binaphtholate ligands, is a more consistent reason for the reduced stability of the δ linkage.

(34) Bachand, B.; Belanger-Gariepy, F.; Wuest, J. D. *Organometallics* 1990, 9, 2860.

(35) (a) Brintzinger, H. H.; Schnutenhaus, H. *Angew. Chem., Int. Ed. Engl.* 1979, 18, 777. (b) Wild, F. R. W. P.; Zsolnai, L.; Huttner, G.; Brintzinger, H. H. *J. Organomet. Chem.* 1982, 232, 233.

(36) (a) Mashima, K.; Kuano, K.; Ohta, T.; Noyori, R.; Takaya, H. *J. Chem. Soc., Chem. Commun.* 1989, 1208. (b) Yamagata, T.; Tani, K.; Tatsuno, Y.; Saito, T. *J. Chem. Soc., Chem. Commun.* 1988, 466. (c) Ohta, T.; Takaya, H.; Noyori, R. *Inorg. Chem.* 1988, 27, 566.

Table VIII. Comparison of Observable Equilibria

starting materials	product	$\Delta H°$, kcal/mol	$\Delta S°$, eu	ΔG_{298}, kcal/mol
[(Me$_2$BINO)Ti(O-i-Pr)$_2$]$_2$ + 2Ti(O-i-Pr)$_4$	2(Me$_2$BINO)Ti$_2$(O-i-Pr)$_6$	−12.5	−38.0	−1.2
{(t-BuMe$_2$Si)$_2$BINO}Ti(O-i-Pr)$_2$ + Ti(O-i-Pr)$_4$	(t-BuMe$_2$Si)$_2$BINO}Ti$_2$(O-i-Pr)$_6$	−12.0	−44.0	+1.1
2(EtO)TiCl$_3$	[(EtO)TiCl$_3$]$_2$	−11.0 (ΔH_f)		ref 18d
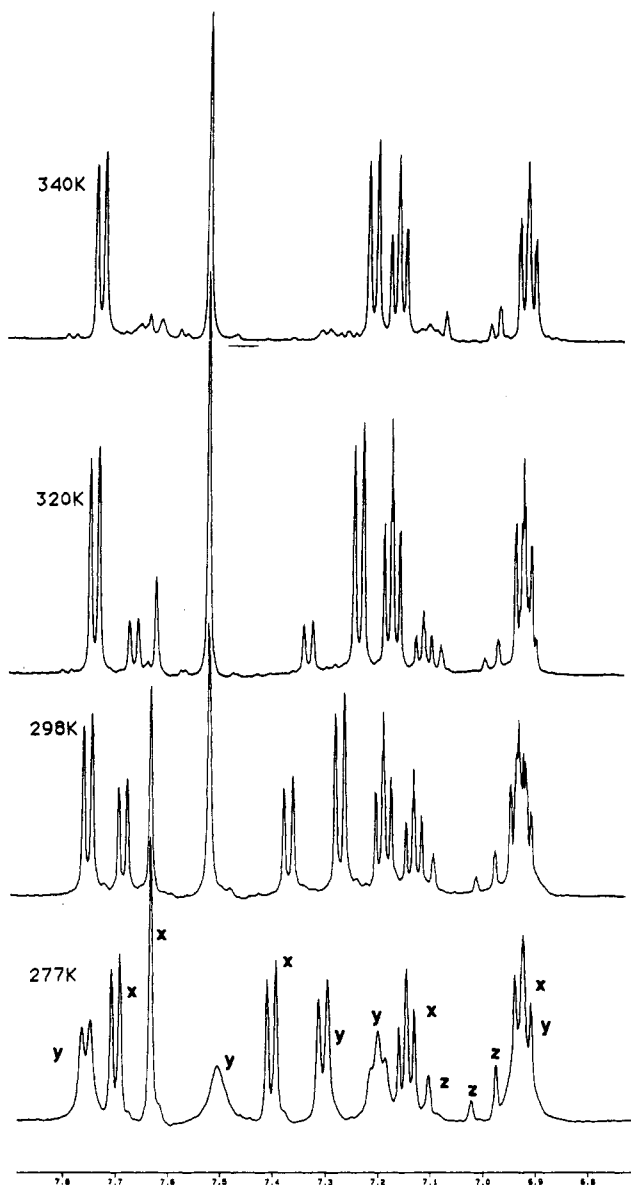
Figure 8. Variable-temperature 500-MHz ^{1}H NMR spectrum (aromatic region) of (Me$_2$BINO)Ti$_2$(O-i-Pr)$_6$, showing an equilibrium between (Me$_2$BINO)Ti$_2$(O-i-Pr)$_6$ and [(Me$_2$BINO)Ti(O-i-Pr)$_2$]$_2$. Resonances representing the following compounds are labeled: x = (Me$_2$BINO)Ti$_2$(O-i-Pr)$_6$, y = [(Me$_2$BINO)Ti(O-i-Pr)$_2$]$_2$, z = toluene-d_8.

Equilibria Involving Mononuclear and Dinuclear Titanium Complexes. Further changes occur in the ^{1}H and ^{13}C NMR spectra of the (Me$_2$BINO)Ti$_2$(O-i-Pr)$_6$ and {(t-BuMe$_2$Si)$_2$BINO}Ti$_2$(O-i-Pr)$_6$ complexes as the samples approach ambient temperature. These variations are consistent with the existence of dynamic equilibria between these complexes and various mono- and dinuclear precursors. Consider the example of the variable-temperature ^{1}H NMR spectrum of (Me$_2$BINO)Ti$_2$(O-i-Pr)$_6$ (Figure 8). As the temperature is increased above 273 K, the naphtholate resonances consistent with the fast-exchange limit of (Me$_2$BINO)Ti$_2$(O-i-Pr)$_6$ diminish without proceeding through classic decoalescence behavior. A new set of naphtholate resonances that exactly correspond to the
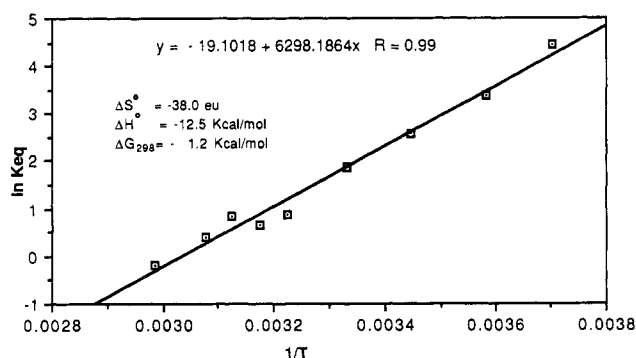

Figure 9. van't Hoff plot of the equilibrium between (Me$_2$BINO)Ti$_2$(O-i-Pr)$_6$ and [(Me$_2$BINO)Ti(O-i-Pr)$_2$]$_2$. Thermodynamic characteristics for the equilibrium determined from the linear regression analysis include $\Delta H°$ = −12.5 ± 0.6 kcal/mol, $\Delta S°$ = −38 ± 2 eu, and $\Delta G°_{298}$ = −1.2 kcal/mol.

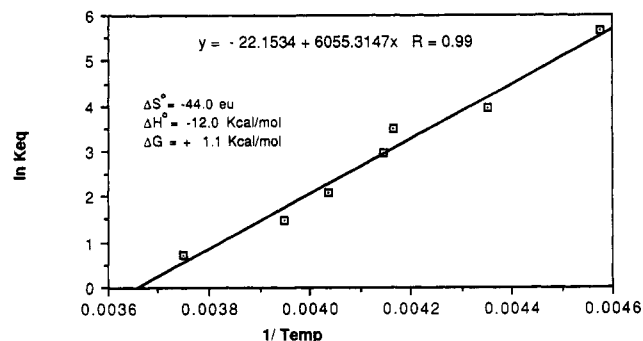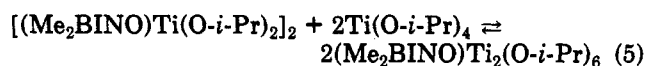**Figure 10.** van't Hoff plot of the equilibrium between {(t-BuMe$_2$Si)$_2$BINO}Ti$_2$(O-i-Pr)$_6$ and {(t-BuMe$_2$Si)$_2$BINO}Ti(O-i-Pr)$_2$. Thermodynamic characteristics for the equilibrium determined from the linear regression analysis include $\Delta H°$ = −12.0 ± 0.8 kcal/mol, $\Delta S°$ = −44 ± 4 eu, and $\Delta G°_{298}$ = +1.1 kcal/mol.

fast-exchange limit of [(Me$_2$BINO)Ti(O-i-Pr)$_2$]$_2$ grow into the spectrum over the same temperature range. Concurrent with the appearance of these and other spectroscopic features of [(Me$_2$BINO)Ti(O-i-Pr)$_2$]$_2$, resonances associated with free Ti(O-i-Pr)$_4$ grow into the spectrum of the reaction mixture. By 337 K, the initial complex has undergone virtually complete conversion to [(Me$_2$BINO)Ti(O-i-Pr)$_2$]$_2$ and Ti(O-i-Pr)$_4$. Decreasing the temperature of the sample exactly reverses the observed spectroscopic changes. This behavior is consistent with the existence of an equilibrium between the two dinuclear Me$_2$BINO-substituted Ti complexes (eq 5). Equilibrium constants modeled on this

$$[(Me_2BINO)Ti(O\text{-}i\text{-}Pr)_2]_2 + 2Ti(O\text{-}i\text{-}Pr)_4 \rightleftharpoons$$
$$2(Me_2BINO)Ti_2(O\text{-}i\text{-}Pr)_6 \quad (5)$$

equation were obtained from variable-temperature NMR studies, and a van't Hoff plot of these data (Figure 9) was used to obtain the thermodynamic constants associated with the equilibrium process. {(t-BuMe$_2$Si)$_2$BINO}Ti$_2$(O-i-Pr)$_6$ participates in a similar equilibrium with {(t-BuMe$_2$Si)$_2$BINO}Ti(O-i-Pr)$_2$ and Ti(O-i-Pr)$_4$ (eq 6).

$$\{(t\text{-}BuMe_2Si)_2BINO\}Ti(O\text{-}i\text{-}Pr)_2 + Ti(O\text{-}i\text{-}Pr)_4 \rightleftharpoons$$
$$\{(t\text{-}BuMe_2Si)_2BINO\}Ti_2(O\text{-}i\text{-}Pr)_6 \quad (6)$$
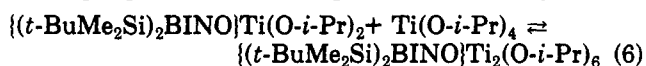
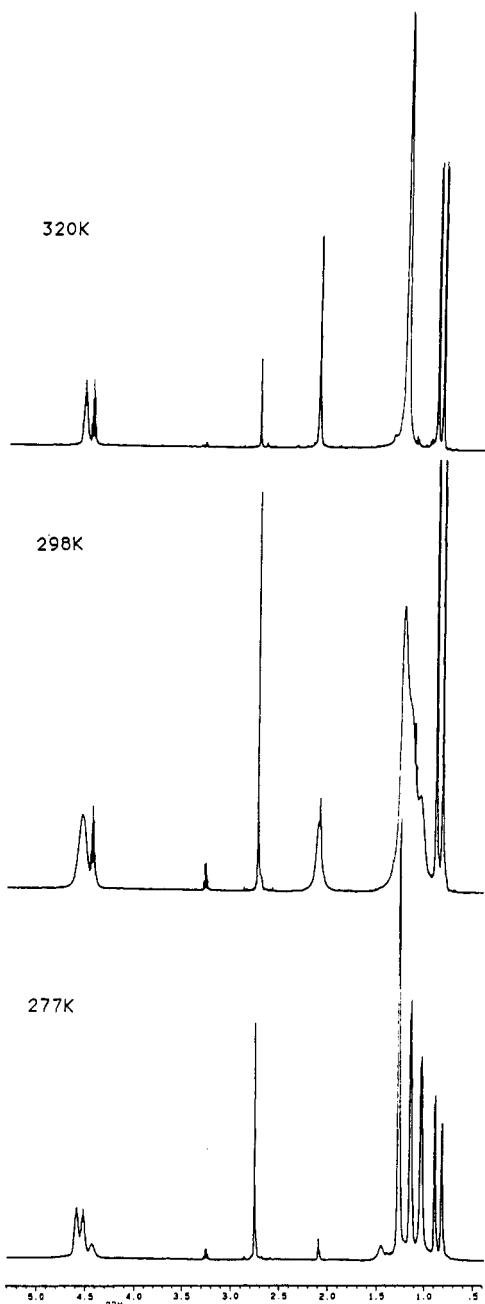Equilibrium constants derived from this NMR study also fit a van't Hoff relationship (Figure 10). The thermody-

Figure 11. Variable-temperature 500-MHz ¹H NMR spectrum of (Me₂BINO)Ti₂(O-*i*-Pr)₆ and Ti(O-*i*-Pr)₄.

Figure 12. Eyring plot of the rate of intermolecular Ti(O-*i*-Pr)₄ exchange in (Me₂BINO)Ti₂(O-*i*-Pr)₆. Activation parameters determined from the plot include $\Delta H^{\ddagger}$ = 14.1 ± 0.9 kcal/mol, $\Delta S^{\ddagger}$ = -2.3 ● 2 eu, and ΔG_{298}(calc) = 14.8 kcal/mol.

namic parameters associated with these equilibria are collected in Table VIII. Similar equilibria, which showed only minor amounts of "disproportionation" of (tartrate)Ti₂(O-*i*-Pr)₆ into Ti(O-*i*-Pr)₄ and (tartrate)₂Ti₂(O-*i*-Pr)₄ were recently reported by Sharpless and Finn.[19]

Isoenergic Intermolecular Titanium Fragment Transfer Processes. A second type of intermolecular exchange process is observed in spectra of (Me₂BINO)-Ti₂(O-*i*-Pr)₆. The ¹H NMR spectrum of an equilibrium mixture generated by dissolving (Me₂BINO)Ti₂(O-*i*-Pr)₆ in toluene-*d*₈ at ambient temperature (Figure 11) clearly shows distinct resonances for the equivalent diastereotopic *i*-PrO groups of (Me₂BINO)Ti₂(O-*i*-Pr)₆ and the non-diastereotopic *i*-PrO ligands of Ti(O-*i*-Pr)₄ (δ = 0.86 and 1.26, respectively). Increasing the temperature of the sample results in a noticeable broadening of these resonances and in their eventual coalescence to a time-averaged doublet at 327 K (δ = 1.20). These observations are consistent with the existence of a mechanism for the isoenergic

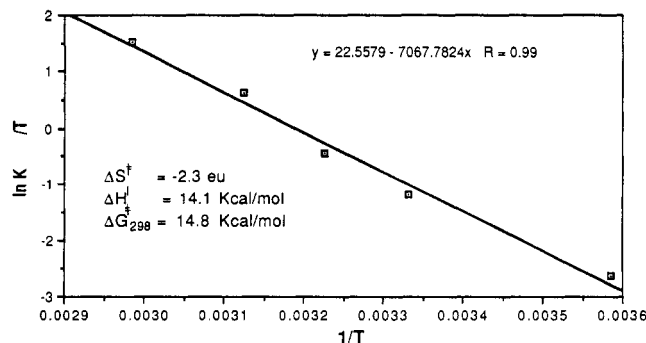exchange of the *i*-PrO ligands of (Me₂BINO)Ti₂(O-*i*-Pr)₆ into the pool of Ti(O-*i*-Pr)₄ generated by the equilibrium between the two dinuclear Ti complexes (eq 7). The onset

$$(R_2BINO)Ti_2(O\text{-}\boldsymbol{i}\text{-}Pr)_6 + Ti(O\text{-}\boldsymbol{i}\text{-}Pr)_4 \rightleftharpoons$$
$$(R_2BINO)Ti_2(O\text{-}\boldsymbol{i}\text{-}Pr)_m(O\text{-}\boldsymbol{i}\text{-}Pr)_{6-m} +$$
$$Ti(O\text{-}\boldsymbol{i}\text{-}Pr)_{4-m}(O\text{-}\boldsymbol{i}\text{-}Pr)_m \quad (7)$$

of the coalescence temperature is reduced by the addition of excess Ti(O-*i*-Pr)₄ to the mixture. A line-shape analysis of this exchange process, which necessarily involved modeling variations in both the line shape and the concentration of the various constituents, yielded rate constants for exchange at several temperatures.[37] Eyring plots of these constants yielded activation parameters ($\Delta H^{\ddagger}$ = 14.1 ± 0.9 kcal/mol, $\Delta S^{\ddagger}$ = -2 ± 2 eu) for the exchange process in the Me₂BINO derivative (Figure 12). The free energy of activation of this intermolecular exchange is substantially larger than the barrier for intramolecular rearrangement of (Me₂BINO)Ti₂(O-*i*-Pr)₆ through the C_2-symmetric intermediate outlined above, confirming that different transition states are involved in the two exchange processes.

Discussion

Structural Considerations. [(Me₂BINO)Ti(O-*i*-Pr)₂]₂. The predisposition of [(Me₂BINO)Ti(O-*i*-Pr)₂]₂ to exist as an R^*,R^* dimer, even when conditions exist for the molecule to adopt a meso-R,S form, bears further comment. This structure type is a consistent feature of bimetallic complexes having a 1,3-dioxadimetallacycle core that bear two bidentate chiral ligands.[33,38] Structurally characterized examples of such complexes include the edge-shared bioctahedral dimer of (N,N'-dibenzyltartramide)Ti(O-*i*-Pr)₂ and the edge-shared bis-tetrahedral dimer of ((N,N-dimethylamino)isoborneate)(Me)Zn.[38] This structure type lends the molecule C_2 symmetry, engendering identical chemical environments at the two metal centers. For complexes containing ligands of like chirality, this skeletal arrangement dictates a syn relationship between the alkyl tethers bound to the bridging alkoxide ligands. In instances where these groups have nonnegligible steric bulk, significant 1,3 trans annular interactions might develop, stabilizing the related C_S-symmetric R,S isomer with respect to the R^*,R^* diastereomer. This behavior is exhibited in (DAB)₂R₂Zn₂ through a 600-fold greater stability constant for the R,S dimer.[38]
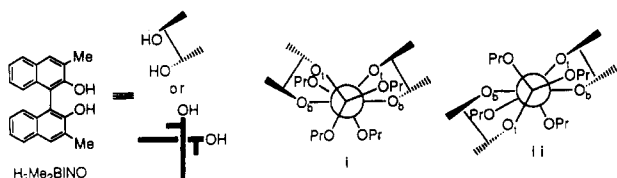
(37) Line-shape analyses were performed on a VAX 6460, using the DNMRH software available from QCPE, Indiana University, Bloomington, IN 47405.

(38) Kitamura, M.; Okada, S.; Suga, S.; Noyori, R. *J. Am. Chem. Soc.* **1989,** *111,* 4028.

Scheme II
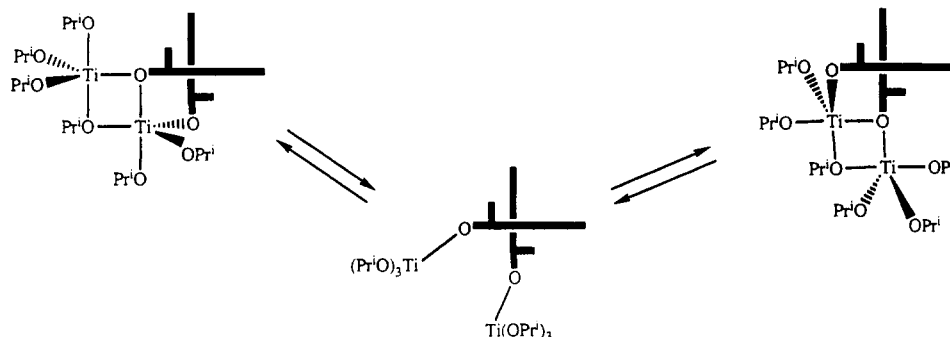
It is reasonable to assume, on the basis of the facile intermolecular ligand-transfer processes noted previously, that the (R^*,R^*)-[(Me$_2$BINO)Ti(O-i-Pr)$_2$]$_2$ complex forms under conditions of a thermodynamically controlled equilibrium. We can effectively rule out π-stacking interactions as the origin of the stability of the R^*,R^* diastereomer, considering that a careful analysis shows the closest approach of the *syn*-naphtholate rings is 3.4 Å. The reason for the preferred cofacial presentation of the naphtholate ligands is most likely steric. Interactions between the *syn*-naphtholate groups are minimized by a combination of the nearly parallel presentation of the "planar" naphtholate groups and the slight distortions from ideal planarity in the Ti-O-Ti-O core. Moreover, the cofacial arrangement of the naphtholate units in the R^*,R^* isomer (i) avoids potentially destabilizing interligand interactions that would be engendered in the alternative R,S diastereomer (ii). In particular, the R^*,R^* structure re-


moves the two gauche interactions between the *syn*-i-PrO and terminal naphtholate ligands.

Intramolecular Rearrangement Processes. Two of the rearrangement processes observed in this study—specifically, the fluxional behavior of [(Me$_2$BINO)Ti(O-i-Pr)$_2$]$_2$ (Figure 1) and the low-temperature equilibration of i-PrO environments in (Me$_2$BINO)Ti$_2$(O-i-Pr)$_6$ (Figure 3)—might occur via strictly intramolecular mechanisms. The exchange of i-PrO environments in (R$_2$BINO)Ti$_2$(O-i-Pr)$_6$ is, almost certainly, an intramolecular process. The independent observation of a higher energy fragmentation mechanism for intermolecular exchange (vide infra) eliminates the only plausible dissociative intermolecular process. Moreover, conceivable intermolecular i-PrO ligand interchange processes, which might occur through bis-i-PrO-bridged tetranuclear species, cannot equilibrate all of the i-PrO environments in a single molecule. The rearrangement process probably occurs through the rupture of the sterically less favorable i-PrO bridge to produce a C_2-symmetric intermediate analogous in structure to {(t-BuMe$_2$Si)$_2$BINO}Ti$_2$(O-i-Pr)$_6$ (Scheme II). Any i-PrO ligand could then reclose the 1,3-dioxadititanacycle, leading to complete exchange of the chemical environments of like ligands.

The rearrangement of the [(Me$_2$BINO)Ti(O-i-Pr)$_2$]$_2$ complex could conceptually occur through two pathways (Scheme III): (a) Fragmentation of the dinuclear complex through the interruption of alkoxide bridges would produce two C_2-symmetric mononuclear fragments (iii), which

Scheme III
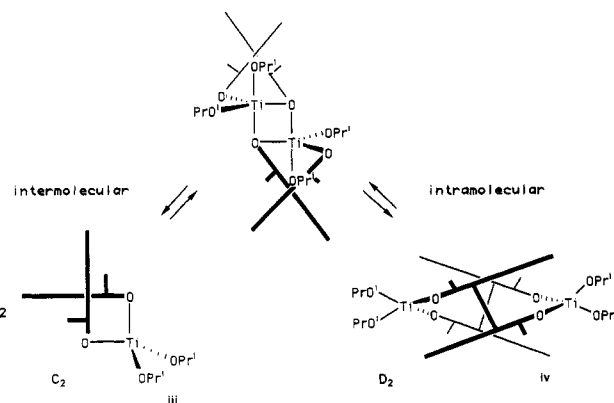
would combine to re-form the initial dinuclear structure. (b) Internal cleavage of Ti-O bonds in a naphthoxide-bridged molecule would lead to a D_2-symmetric dinuclear intermediate (iv) containing nonchelating naphthoxide bridges. Note that the ^{1}H NMR spectrum of this D_2 structure would contain features similar to those of the C_2-symmetric mononuclear fragment. It is difficult to draw a clear distinction between these mechanisms on the basis of the available data. Within the limits of our cryoscopic molecular weight study ($\pm 10\%$), there is no evidence of the presence of substantial mononuclear complex at 279 K, even though the exchange process is already occurring at an appreciable rate at this temperature. The entropic term for this exchange process ($\Delta S^\ddagger = +10$ eu), while not consistent with significant degree of bimolecular character at the transition state, is sufficiently positive by comparison with other intermolecular exchange processes (vide infra) to suggest that the molecule could be rearranging through the fragmentation pathway. In contrast, the intramolecular exchange pathway in Scheme III closely corresponds to a mechanism for intramolecular exchange in [(tartrate)Ti(O-i-Pr)$_2$]$_2$ proposed by Sharpless and Finn.[19] While the participation of a dimer–monomer equilibrium at higher temperatures cannot at present be completely discounted, we propose, based on analogy to the mechanism of Sharpless, that the exchange occurs through highly organized intramolecular bond cleavage to produce a bis-Me$_2$BINO-bridged dinuclear intermediate.

Intermolecular Rearrangement Processes. Two chemically distinct pathways for intermolecular rearrangement have been identified in this study: (1) equilibria between chemically distinct compounds, which are observable through direct measurement of the chemical species, and (2) isoenergic exchange processes, which are detectable through coalescence behavior. Conceptually, each of these processes could occur through either intermolecular ligand exchange or the transfer of complete "Ti(OR)$_4$" units. For the equilibrium involving {(t-

BuMe$_2$Si)$_2$BINO}Ti$_2$(O-i-Pr)$_6$, this distinction is academic, as the molecule indisputably rearranges through two mononuclear titanium fragments. It is also reasonable to assume that the equilibrium between [(Me$_2$BINO)Ti(O-i-Pr)$_2$]$_2$ and (Me$_2$BINO)Ti$_2$(O-i-Pr)$_6$, which involves Ti(O-i-Pr)$_4$, proceeds via titanium fragment exchange and not through ligand redistribution between [(Me$_2$BINO)Ti(O-i-Pr)$_2$]$_2$ and "Ti$_2$(O-i-Pr)$_8$".

The mechanism of intermolecular exchange involving Ti(O-i-Pr)$_4$ and (Me$_2$BINO)Ti$_2$(O-i-Pr)$_6$ is less straightforward. In addition to a simple dissociative mechanism for Ti(O-i-Pr)$_4$ fragment exchange, the observed rearrangement process could also be explained through an associative process involving either the pairwise exchange of i-PrO ligands or the exchange of entire Ti(O-i-Pr)$_4$ units. These associative mechanisms are suspect in light of the small magnitude of the observed activation entropy (−2 ± 2 eu). Some point of reference was established by the monomer–dimer equilibrium between W$_2$(O-i-Pr)$_6$ and W$_4$(O-i-Pr)$_{12}$, which displays $\Delta S^{\ast}$ terms of −39 eu for an associative transition state and +18 eu for a dissociative transition state.[39] Based on this precedent, it also seems unlikely that the rate-determining step in the intermolecular exchange between (Me$_2$BINO)Ti$_2$(O-i-Pr)$_6$ and Ti-(O-i-Pr)$_4$ (eq 7) is a full-fledged cleavage of the complex into two mononuclear fragments. It is more probable that the rate-limiting step in this exchange process involves the disruption of a bond in (Me$_2$BINO)Ti$_2$(O-i-Pr)$_6$ that leaves the stoichiometry of the complex unchanged but generates an intermediate that is susceptible to rapid Ti(O-i-Pr)$_4$ exchange. If we examine the ligand environments in (Me$_2$BINO)Ti$_2$(O-i-Pr)$_6$, it is clear that this intramolecular cleavage process can only involve the bridging ligands (μ-O-i-Pr or μ-ONap). Rupture of the isopropoxide bridge bond leads to the C_2-symmetric complex (Scheme II), previously identified as the intermediate responsible for the equilibration of all of the i-PrO environments in (Me$_2$BINO)Ti$_2$(O-i-Pr)$_6$. Intramolecular ligand exchange through this intermediate has a $\Delta G^{\ast}_{240}$ of 10.8 kcal/mol and is distinct from the intermolecular exchange between (Me$_2$BINO)$_2$Ti$_2$(O-i-Pr)$_6$ and Ti(O-i-Pr)$_4$, which has a $\Delta G^{\ast}_{240}$ of 14.6 kcal/mol. Consequently, the rate-determining step for intermolecular Ti(O-i-Pr)$_4$ fragment exchange must be the disruption of a naphthoxide bridging interaction. The free energy difference ($\Delta\Delta G^{\ast}_{240}$) of −3.8 kcal/mol between these intramolecular and intermolecular exchange processes represents the greater stability of the less sterically encumbered naphthoxide bridge.

Thermodynamics of Polynuclear Aggregation. This study has uncovered two instances of equilibria in which two or more precursor molecules aggregate to form dinuclear complexes. As expressed in the form shown in eqs 5 and 6, the equilibria would be expected to have large negative $\Delta S°$ terms, consistent with a net reduction in the number of molecules in solution (Table VII). The observed entropic values of −38 ± 2 and −44 ± 4 eu, respectively, are fully consistent with this expectation. The magnitude and sign of the $\Delta H°$ and $\Delta S°$ values set the two terms in the free energy expression in opposition, resulting in the prevalence of the reactants above 40 °C and the products below 0 °C. Marsi has noted similarly small values for the ΔG_{298} of a monomer–dimer equilibrium in a titanium transesterification catalyst.[6b]

When considered in a simplistic manner, the similar magnitudes of the $\Delta H°$ terms for the equilibria (eqs 5 and 6) are initially somewhat troubling. The observed $\Delta H°$

values are clearly substantially less than the heat of formation of a Ti–O single bond. Furthermore, the equilibrium that ultimately results in the formation of two new Ti–O bonding interactions (eq 5) has virtually the same enthalpic term as the process that results in the net formation of no new bonds between titanium and oxygen (eq 6). The only previous rigorous estimate of the enthalpy of alkoxide bridge formation in titanium alkoxide complexes showed a ΔH_f of −11 kcal/mol and grew out of a careful study of dynamic ligand exchange, molecular weight cryoscopy, and calorimetric experiments in ethoxide-containing Ti complexes.[18d] The only shortcoming of this study was the lack of solution-phase structural information about the polynuclear alkoxides under investigation. Still, this value is identical within experimental error of the $\Delta H°$ of −12 kcal/mol we have observed for the formation of two different dinuclear titanium compounds in this study. That such divergent reactions—differing in the steric demands of the ligands, structural characteristics of the products, and numbers of bonds broken and made and similar only in that each results in the formation of a single new dinuclear Ti complex—should possess similar $\Delta H°$ values is remarkable. These results indicate that many of the "simple" electronic and steric effects that might be considered to control the favorability of specific aggregation processes frequently engage in such a subtle interplay that efforts to use them in a predictive manner are fruitless. More information is required to determine whether the principles of these nucleation processes can be generalized across the range of the group 4 elements.

Conclusions

The results of this study define several important characteristics of exchange processes involving titanium alkoxide complexes:

(1) The central structural characteristics of dinuclear titanium complexes containing chiral bidentate ligands are similar over a wide range of complexes. This similarity extends even to the structures of intermediates involved in ligand exchange.

(2) A specific dinuclear titanium complex may engage in distinct intramolecular and intermolecular rearrangement processes. The activation parameters of these processes have, in at least one case, defined independent intramolecular and dissociative intermolecular exchange pathways.

(3) Titanium alkoxide derivatives participate in facile equilibria involving the interconversion of chemically distinct compounds. The enthalpic terms in these equilibria favor aggregation into higher nuclearity alkoxides, while entropic factors detract from the favorability of these reactions.

(4) Complexes engaging in such equilibria may also be involved in separate isoenergic rearrangement processes, through exchange of their constituent "Ti(OR)$_4$" units with a pool of free "Ti(OR)$_4$".

(5) Intermolecular exchange processes can possess nearly zero activation entropies, indicating that the transition states for these reactions may involve intramolecular bond reorganization. The most likely course of these processes is the disruption of an alkoxide bridge, resulting in a monobridged dititanium intermediate at which "Ti(OR)$_4$" exchange is extremely rapid.

(6) The enthalpic gain from the formation of a dinuclear titanium complex in a molecular aggregation process is approximately 12 kcal/mol.

These insights highlight the intricacy of titanium alkoxide coordination chemistry. They also clearly define

(39) Chisholm, M. H.; Clark, D. L.; Hampden-Smith, M. J. *J. Am. Chem. Soc.* **1989**, *111*, 4028.

some potential difficulties that may be encountered in employing polynuclear titanium alkoxides as catalysts for organic reactions. Future studies in our laboratory will be directed toward the elaboration of the thermodynamics and kinetics of formation of other fundamental subunits in polynuclear group 4 complexes.

Experimental Section

All reactions were carried out under a prepurified nitrogen atmosphere, using standard Schlenk techniques unless otherwise stated. Solvents were dried by conventional methods and freshly distilled under nitrogen. NMR solvents were dried over 5-Å molecular sieves and degassed with a dry N_2 purge prior to use. ^1H and ^{13}C NMR spectra were obtained on a Varian XL 300-MHz or a Bruker AM 500-MHz spectrometer. ^1H NMR spectra were referenced against the residual proton impurity in benzene-d_6, toluene-d_8, acetone-d_6, or chloroform-d_1 while ^{13}C NMR spectra were referenced against the resonances representing the aromatic carbons of benzene-d_6, the aromatic carbons or the methyl group carbons of toluene-d_8, and the methyl group carbons of acetone-d_6 or chloroform-d_1. Mass spectra were obtained on a Ribermag MS10, using a direct insert source under a constant purge of argon. Elemental analyses were performed by Desert Analytics, P.O. Box 41838, Tucson, AZ 85717, or Schwarzkopf Microanalytical Laboratory 56-19 27th Ave., Woodside, NY 11377. Cryoscopic molecular weight determinations were performed in benzene. Ti-(O-i-Pr)$_4$ (Aldrich), 2,2′-dihydroxy-1,1′-binaphthyl (H$_2$BINO), and (+)-(R)-2,2′-dihydroxy-1,1′-binaphthyl ((+)-R-H$_2$BINO) (Kodak) were used as purchased. 3,3′-Dimethyl-2,2′-dihydroxy-1,1′-binaphthyl (H$_2$Me$_2$BINO and (+)-R-H$_2$Me$_2$BINO), 3,3′-diphenyl-2,2′-dihydroxy-1,1′-binaphthyl (H$_2$Ph$_2$BINO), 3,3′-(*tert*-butyldimethyl)-2,2′-dihydroxy-1,1′-binaphthyl (H$_2$(t-BuMe$_2$Si)$_2$BINO), and 3,3′-dibromo-2,2′-dihydroxy-1,1′-binaphthyl (H$_2$Br$_2$BINO) were prepared by slight alterations of literature methods.

[(Me$_2$BINO)Ti(O-i-Pr)$_2$]$_2$. H$_2$Me$_2$BINO (1.5 g, 4.8 mmol) and diethyl ether (125 mL) were introduced into a Schlenk flask (250 mL). Ti(O-i-Pr)$_4$ (1.4 mL, 4.0 mmol) was added via syringe, producing a yellow-orange solution. After 10 min, the solvent was removed in vacuo and the resulting yellow solid was washed twice with a minimum of cold pentanes to remove unreacted Ti(O-i-Pr)$_4$. The residual material was dissolved in a minimum volume of diethyl ether and the resultant solution refrigerated at −20 °C. Large orange crystals of [(Me$_2$BINO)Ti(O-i-Pr)$_2$]$_2$ which clouded upon drying under vacuum were isolated (yield 90%). Isolation of this powder from hexanes in a similar manner produced X-ray quality crystals. ^1H NMR (300 MHz, benzene-d_6, 20 °C): δ 7.54 (2 H, d, Me$_2$BINO), 7.80, 7.74, (2 H, d, J = 4.7 Hz, Me$_2$BINO), 7.22, 6.96 (2 H, t, J = 4.9 Hz, Me$_2$BINO), 2.15 (6 H, bs, Me$_2$BINO), 4.44 (2 H, sept, J = 5.4 Hz, OCH*Me*$_2$), 0.89, 0.87 (3 H, d, J = 5.1 Hz, OCH*Me*$_2$). ^1H NMR (500 MHz, toluene-d_8, −50 °C): δ 7.86 (2 H, d, J = 5.0 Hz, Me$_2$BINO), 7.75 (2 H, d, J = 5.0 Hz, Me$_2$BINO), 7.62 (2 H, s, Me$_2$BINO), 7.48 (2 H, d, J = 5.0 Hz, Me$_2$BINO), 7.4–7.1 (m, solvent and Me$_2$BINO), 7.01 (2 H, s, Me$_2$BINO), 6.81 (2 H, t, J = 5.0 Hz, Me$_2$BINO), 4.61 (2 H, sept, *CH*(CH$_3$)$_2$), 4.26 (2 H, sept, *CH*(CH$_3$)$_2$), 2.99 (3 H, s, *Me*$_2$BINO), 1.31 (3 H, s, *Me*$_2$BINO) 1.0–0.6 (m, CH(*CH$_3$*)$_2$). ^{13}C NMR (500 MHz, toluene-d_8, 20 °C): δ 160.5, 132.2, 130.7, 129.9, 129.6, 123.9, 118.8 (BINO), 80.9 (O*CH*Me$_2$), 25.4 (*Me*$_2$BINO), 18.4 (OCH*Me*$_2$). ^{13}C{^1H} NMR (500 MHz, toluene-d_8, −50 °C): δ 159.6, 137.1, 132.6, 130.7, 130.1, 130.0, 129.9, 127.2, 126.7, 124.2, 123.2, 120.0, 116.5 (Me$_2$BINO), 81.3, 80.4 (O*CH*Me$_2$), 25.7, 25.5, 25.3, 24.9 (OCH*Me*$_2$). Molecular weight (benzene, ca. 6 °C): calcd, 956; found, 991 ± 95. Anal. Calcd: C, 70.13; H, 6.32. Found: C, 70.30; H, 6.32.

(Me$_2$BINO)Ti$_2$(O-i-Pr)$_6$. In a Schlenk flask (25 mL), [(Me$_2$BINO)Ti(O-i-Pr)$_2$]$_2$ (0.5 g, 1.1 mmol) was dissolved in toluene (15 mL). Ti(O-i-Pr)$_4$ (0.311 mL, 1.1 mmol) was added via syringe. The reaction was left to stir for 30 min, and then the solvent was removed in vacuo. Refrigeration in a minimum volume of hexane at −20 °C produced yellow microcrystals. Yield: crystalline, 48–50%. ^1H NMR (500 MHz, toluene-d_8, 200 K, *crystals were dissolved at dry ice temperatures and left to warm to 200 K in the NMR cavity*): δ 7.78 (2 H, Me$_2$BINO), 7.63 (1 H, s, Me$_2$BINO), 7.59 (3 H, m, Me$_2$BINO), 7.50 (1 H, d, J = 8.0 Hz, Me$_2$BINO), 7.23 (2 H, m, Me$_2$BINO), 6.90 (1 H, m, Me$_2$BINO), 4.99, 4.92, 4.80, 4.00, 3.95 (1 H, b, sept, OCH*Me*$_2$), 2.98, 2.70 (3 H, *Me*$_2$BINO),

1.65, 1.53, 1.47, 1.30, 1.11, 0.99, 0.92, 0.88, 0.75, 0.67, 0.48 (3 H, bd, OCH*Me*$_2$). Mass spectrometry: m/e = 479 ((Me$_2$BINO)-Ti(O-i-Pr)$_2$$^+$), 377 (Me$_2$BINO)TiO$^+$). Molecular weight: calcd, 762 (fully associated) or 508 (fully dissociated); found, 506 ± 95. Anal. Calcd: C, 62.84; H, 7.42. Found: C, 62.99; H, 7.06.

(Me$_2$BINO)$_2$Ti. In a Schlenk flask (25 mL), Li$_2$Me$_2$BINO (0.3 g, 0.92 mmol), prepared via the reaction of n-BuLi and H$_2$Me$_2$BINO in diethyl ether, was slurried in diethyl ether (15 mL). The flask was then cooled to −78 °C, and TiCl$_4$ was syringed onto this mixture. The solution immediately turned dark orange. The solution was allowed to warm to room temperature, the mixture was filtered, and the filtrate was concentrated. Cooling at −20 °C produced orange microcrystals. ^1H NMR (20 °C, 500 MHz, toluene-d_8): δ 7.61 (Me$_2$*BINO*, d, 2 H, J = 4.1 Hz), 7.15 (Me$_2$*BINO*, t, 2 H, J = 7.7 Hz), 7.08 (Me$_2$*BINO*, s, 2 H), 6.83 (Me$_2$*BINO*, d, 2 H, J = 4.2 Hz), 6.74 (Me$_2$*BINO*, t, 2 H, J = 4.3 Hz), 1.61 (*Me*$_2$BINO, 3 H).

{(t-BuMe$_2$Si)$_2$BINO}Ti(O-i-Pr)$_2$. In a Schlenk flask (25 mL), H$_2$(t-BuMe$_2$Si)$_2$BINO (0.4 g, 0.775 mmol) was dissolved in toluene. Ti(O-i-Pr)$_4$ (0.23 mL, 0.775 mmol) was added by syringe, producing a bright yellow solution. The mixture was refluxed for 24 h and then cooled to room temperature. The solvent was removed in vacuo, and the residue was redissolved in pentanes. The volume of the solution was drastically reduced and cooled to −20 °C. This results in clear yellow microcrystals. Yield: 61%. ^1H NMR (300 MHz, CDCl$_3$, 20 °C): δ 7.99 (2 H, s, BINO), 7.79 (2 H, d, BINO, J = 4.2 Hz), 7.23 (2 H, t, BINO, J = 6.9 Hz), 7.07 (2 H, t, BINO, J = 7.0 Hz), 6.76 (2 H, d, BINO, J = 7.0 Hz), 4.39 (2 H, sept, OCH(CH$_3$)$_2$, J = 6.2 Hz), 1.14 (6 H, d, OCH(*CH$_3$*)$_2$, J = 2.9 Hz), 1.02 (6 H, d, OCH(*CH$_3$*)$_2$, J = 2.9 Hz), 0.88 (18 H, s, SiC(*CH$_3$*)$_3$)), 0.49 (6 H, s, Si(*Me*)$_2$) 0.42 (6 H, s, Si(*Me*)$_2$). ^{13}C{^1H} NMR (300 MHz, toluene-d_8, 20 °C): δ 160.4, 139.9, 138.9, 136.1, 130.3, 128.8, 127.2, 124.0, 118.3 (partial BINO), 80.5 (O*CH*(CH$_3$)$_2$), 30.4 (Si*C*-(CH$_3$)$_3$), 27.5 (SiC(*CH$_3$*)$_3$), 26.0 (SiC(*CH$_3$*)$_3$), 27.5 (Si*C*(*CH$_3$*)$_3$, 26.0 (SiC(*CH$_3$*)$_3$), 25.8 (OCH(*CH$_3$*)$_2$), −2.61 (Si(*Me*)$_2$), −4.31 (Si(*Me*)$_2$. Mass spectrometry: m/e = 678 [{(t-BuMe$_2$Si)$_2$BINO}Ti(O-i-Pr)$_2$], 621 [{(t-BuMe$_2$Si)(Me$_2$Si)BINO}Ti(O-i-Pr)$_2$], 579 [{(t-BuMeSi)-(Me)}BINO)Ti(O-i-Pr)$_2$], 563 [{(t-BuMe$_2$Si)BINO}Ti(O-i-Pr)$_2$], 521 [{(Me$_2$SiBINO}Ti(O-i-Pr)$_2$], 463 [{(Me)BINO}Ti(O-i-Pr)$_2$], 448 [{BINO}Ti(O-i-Pr)$_2$]. Anal. Calcd: C, 67.22; H, 8.02. Found: C, 66.51; H, 7.86.

{(t-BuMe$_2$Si)$_2$BINO}Ti$_2$(O-i-Pr)$_6$. In a round-bottom Schlenk flask, H$_2$(t-BuMe$_2$Si)$_2$BINO (0.47 g, 0.914 mmol) was dissolved in toluene. Ti(O-i-Pr)$_4$ (0.54 mL, 1.90 mmol) was syringed onto this solution, resulting in a dark orange solution. The solvent was removed in vacuo, the yellow residue was redissolved in pentanes, and the volume was drastically reduced. Cooling to −20 °C produced yellow crystals. Yield: 0.62 g, 71%. ^1H NMR (300 MHz, CDCl$_3$, 20 °C): δ 7.99 (2 H, s, BINO), 7.79 (2 H, d, BINO, J = 4.0 Hz), 7.23 (2 H, t, BINO, J = 7.0 Hz), 7.07 (2 H, t, BINO, J = 7.0 Hz), 4.51–4.37 (6 H, mult, O*CH*(CH$_3$)$_2$) 1.23 (24 H, d, OCH(*CH$_3$*)$_2$, J = 3.1), 1.14 (6 H, d, OCH(*CH$_3$*)$_2$, J = 3.1), 1.01 (6 H, d, OCH(*CH$_3$*)$_2$, J = 3.1), 0.88 (18 H, s, SiC(*CH$_3$*)$_3$), 0.49 (6 H, s, Si(CH$_3$)$_2$), 0.42 (6 H, s, Si(*CH$_3$*)$_2$). ^{13}C{^1H} NMR (500 MHz, toluene-d_8, 20 °C): δ 160.3, 138.8, 136.1, 130.2, 128.7, 128.4, 128.2, 127.1, 123.9, 118.2 (BINO partial), 80.4 (OCH(CH$_3$)$_2$), 76.4 (O*C*-H(CH$_3$)$_2$), 30.3 (Si*C*(CH$_3$)$_3$), 27.8 (OCH(*CH$_3$*)$_2$, 27.7 (OCH(*CH$_3$*)$_2$), 27.4 (Si*C*(*CH$_3$*)$_3$), 26.7 (OCH(*CH$_3$*)$_2$), −2.62, −4.32 (Si(Me)$_2$). Molecular weight (benzene, ca. 6 °C): calcd, 963 (482 for fully dissociated dimer); found, 577 ± 86. Anal. Calcd: C, 62.35; H, 8.58. Found: C, 62.60; H, 8.58.

Crystallographic Studies. The same general procedures were followed during the crystallographic analyses of the molecular structures of {(t-BuMe$_2$Si)$_2$BINO}Ti(O-i-Pr)$_2$, [(Me$_2$BINO)Ti(O-i-Pr)$_2$]$_2$, and {(t-BuMe$_2$Si)$_2$BINO}Ti$_2$(O-i-Pr)$_6$: Suitable crystals were mounted on a glass fiber using epoxy glues in a glovebag under dry nitrogen. The glass fiber and goniometer head were transferred into a sealed jar and transported to the precooled instrument. The crystal was immediately immersed into a nitrogen jet at 113 K, and centering adjustments were made. All measurements were performed on a Rigaku AFC5R diffractometer with graphite-monochromated Cu Kα radiation employing a 12-kW rotating anode. The data were collected at 113 ± 1 K, using the ω–2θ scan technique to a maximum 2θ of 100.1°. ω scans of several intense reflections, made prior to data collection, showed an average width at half-height of 0.42° (0.53° for

Table IX. Summary of Crystal Data for {(t-BuMe$_2$Si)$_2$BINO}Ti(O-i-Pr)$_2$ (A), [(Me$_2$BINO)Ti(O-i-Pr)$_2$]$_2$ (B), and {(t-BuMe$_2$Si)$_2$BINO}Ti$_2$(O-i-Pr)$_6$ (C)

data	A	B	C
empirical formula	TiO$_4$Si$_2$C$_{37}$H$_{56}$	Ti$_2$O$_8$C$_{56}$H$_{60}$	Ti$_2$Si$_2$O$_8$C$_{50}$H$_{82}$
color of cryst, habit	yellow, prism	yellow, prism	yellow, prism
cryst dimens, mm	0.020 × 0.020 × 0.050	0.100 × 0.100 × 0.300	0.400 × 0.400 × 0.400
space group, system	$P2_1/c$	$P2_1/c$	$C2/c$
lattice parameters			
a, Å	10.866 (3)	17.728 (3)	14.444 (2)
b, Å	15.572 (4)	11.079 (4)	18.676 (3)
c, Å	23.059 (4)	26.232 (4)	20.788 (4)
β, deg	93.76 (2)	101.00 (3)	93.76 (2)
Z, molecules/cell	4	4	4
V, Å^3	3856 (1)	5058 (6)	5596 (3)
d(calcd), g/cm^3	1.152	1.257	1.143
X-ray radiation	Cu Kα (λ = 1.541 78 Å)	Cu Kα	Cu Kα
MW	668.92	956.89	963.16
linear abs coeff, cm^{-1}	27.5	31.07	32.1
scan speed, deg/min	16.0	4.0	32.0
scan width, deg + dispersion	1.15 + 0.30 tan θ	1.15 + 0.30 tan θ	1.89 + 0.30 tan θ
bkgd count: peak count	1:2	1:2	1:2
aperature size (vert × horiz), mm	6.0 × 6.0	6.0 × 6.0	6.0 × 6.0
2θ max, deg	100.1	100.1	112.7
total no. of reflcns collected	4441	5762	4015
no. of unique intens	4162	5537	3833
$R(F)$	0.037	0.068	0.059
$R_w(F)$	0.051	0.078	0.091
goodness of fit for last cycle	1.54	1.39	1.59
Δ/σ for last cycle	0.42	0.86	0.82
temp, K	113	106	113

[(Me$_2$BINO)Ti(O-i-Pr)$_2$]$_2$), with a takeoff angle of 6.0°. Scans were made at a speed of 4.0°/min (in ω) (16.0°/min for [(Me$_2$BINO)Ti(O-i-Pr)$_2$]$_2$). Weak reflections ($I < 10.0\sigma$ (I)) were rescanned (minimum of one recount), and the counts were accumulated to assure good counting statistics. The structures were solved by direct methods. Hydrogen atoms were included in the structure factor calculations in idealized positions (d_{CH} = 0.95 Å) and were assigned isotropic thermal parameters that were 20% greater than the B(eq) value of the atom to which they were bonded. The final cycle of full-matrix least-squares refinement was converged with unweighted and weighted agreement factors of $R = \sum ||F_o| - |F_c||/\sum |F_o|$ and $R_w = [(\sum w(|F_o| - |F_c|)^2/\sum wF_o^2)]^{1/2}$. Neutral atom scattering factors were taken from Cromer and Waber.[40] Anomalous dispersion effects were included in F_c; the values of $\Delta f'$ and $\Delta f''$ were those of Cromer.[40] All calculations were performed using the TEXSAN crystallographic software package of Molecular Structure Corp. Details of the structure refinements are outlined in Table IX and in the discussion below.

{(t-BuMe$_2$Si)$_2$BINO}Ti(O-i-Pr)$_2$. Cell constants and an orientation matrix for data collection were obtained from a least-squares refinement using 25 centered reflections in the range 69.49 < 2θ < 70.03°. The cell was found to be monoclinic. Systematic absences at $h0l$ for $l \neq 2n + 1$ and $0k0$ for $k \neq 2n + 1$ and the successful solution and refinement of the structure defined the space group as $P2_1/c$ (No. 14). Of the 4441 reflections collected, 4162 were unique (R_{int} = 0.026). The intensities of three representative collections, measured after every 150 reflections, remained constant throughout the data collection, indicating that no decay correction was required. The linear absorption coefficient for Cu Kα is determined to be 27.5 cm^{-1}. An empirical absorption correction, based on azimuthal scans of several reflections, was applied. The resulting transmission factors ranged from 0.91 to 1.00. These data were corrected for Lorentz and polarization effects. All non-hydrogen atoms were anisotropically refined. The final refinement, based on 3861 observed reflections ($I > 0.01\sigma(I)$) and 622 variable parameters, converged with R = 0.037 and R_w = 0.051. The largest parameter shift in the final cycle was 0.42 times its esd. This standard deviation of an observation of unit weight was 1.54. The weighting scheme was based on counting statistics and included a factor (p = 0.05) to downweight the intense reflections. Plots of $\sum w(|F_o| - |F_c|)^2$ versus $|F_o|$, reflection order in data collection, (sin θ)/λ, and various classes of indices

show no unusual trends. The maximum and minimum peaks in the final difference Fourier map corresponded to 0.35 and -0.24 e$^-$ Å^{-3}, respectively.

[(Me$_2$BINO)Ti(O-i-Pr)$_2$]$_2$. Cell constants and an orientation matrix for data collection were obtained from a least-squares refinement using 19 centered reflections in the range 67.90 < 2θ < 69.71°. The cell was found to be monoclinic. Systematic absences at $h0l$ for $l \neq 2n + 1$ and $0k0$ for $k \neq 2n + 1$ and the successful solution and refinement of the structure defined the space group $P2_1/c$ (No. 14). Of the 5762 reflections collected, 5537 were unique (R_{int} = 0.071). The intensities of three representative reflections, measured after every 150 reflections, remained constant throughout the data collection, indicating that no decay correction was required. The linear absorption coefficient for Cu Kα is determined to be 31.1 cm^{-1}. Azimuthal scans of several reflections indicated no need for an absorption correction. These data were corrected for Lorentz and polarization effects. All non-hydrogen atoms were anisotropically refined except for the β-carbon atom positions of the isopropoxy ligands (corresponding to the β-carbons bound to O(4), O(5), O(7), and O(8)), because they developed negative thermal parameters during anisotropic refinement. The final refinement, based on 3231 observed reflections ($I > 0.01\sigma(I)$) and 547 variable parameters, converged with R = 0.066 and R_w = 0.077. The largest parameter shift in the final cycle was 0.61 times its esd. The standard deviation of an observation of unit weight was 2.63. The weighting scheme was based on counting statistics, and included a factor (p = 0.03) to downweight the intense reflections. Plots of $\sum w(|F_o| - |F_c|)^2$ versus $|F_o|$, reflection order in data collection, (sin θ)/λ, and various classes of indices show no unusual trends. The maximum and minimum peaks in the final difference Fourier map corresponded to 0.55 and -0.39 e$^-$ Å^{-3}, respectively.

{(t-BuMe$_2$Si)$_2$BINO}Ti$_2$(O-i-Pr)$_6$. Cell constants and an orientation matrix for data collection were obtained from a least-squares refinement using 25 centered reflections in the range 48.02 < 2θ < 49.47°. The cell was found to be monoclinic. Systematic absences at hkl for $h + k \neq 2n + 1$ and $h0l$ for $l \neq 2n + 1$ and the successful solution and refinement of the structure defined the space group $C2/c$ (No. 15). Of the 4015 reflections collected, 3833 were unique (R_{int} = 0.109). The intensities of three representative reflections, measured after every 150 reflections, remained constant throughout the data collection, indicating that no decay correction was required. The linear absorption coefficient for Cu Kα radiation (λ = 1.5418 Å) is determined to be 31.2 cm^{-1}. An empirical absorption correction using the program DIFABS resulted in transmission factors ranging from 0.3941 to 1.000.

(40) Cromer, D. T.; Waber, J. T. *International Tables for X-ray Crystallography*; Kynoch Press: Birmingham, England, 1974; Vol. IV.

These data were corrected for Lorentz and polarization effects. The structure was solved by Patterson methods. All non-hydrogen atoms were anisotropically refined. The *i*-Pr groups attached to O(2) and O(3) were found to be disordered. The occupancy factors of C(19A) and C(19B) and of C(22A) and C(22B) are set to 0.5. These positions were refined anisotropically, although the positional and thermal parameters were refined individually. Hydrogen atoms attached to C(17), C(18), C(19A), C(19B), C(20), C(21), C(22A), C(22B), C(24), and C(25) are not included in the refinement. Hydrogen atoms that have noted esd's in the positional parameter table were refined isotropically, while only the isotropic thermal parameters of the remaining hydrogens were refined. The final refinement, based on 2860 observed reflections ($I > 3.00\sigma(I)$) and 346 variable parameters, converged with $R = 0.059$ and $R_w = 0.091$. The largest parameter shift in the final cycle was 0.82 times its esd. The goodness of fit is 1.59. The weighting scheme was based on counting statistics and included a factor ($p = 0.10$) to downweight the intense reflections. The maximum and minimum peaks in the final difference Fourier map

corresponded to 0.41 and −0.29 e⁻ Å⁻³, respectively.

Supplementary Material Available: Full experimental details of the X-ray structural studies including tables of positional parameters, anisotropic vibrational parameters, bond distances and angles involving non-hydrogen atoms, and bond distances and angles involving hydrogen atoms (57 pages); listings of observed and calculated structure factors (87 pages). Ordering information is given on any current masthead page.

Preparation of Vinylideneruthenium Complexes Promoted by Hemilabile Chelating Phosphine Ligands[1]

Helmut Werner,* Arthur Stark, Michael Schulz, and Justin Wolf

Institut für Anorganische Chemie der Universität Würzburg, Am Hubland, D-8700 Würzburg, Germany

The octahedral ruthenium(II) complexes [RuCl₂(P⌒O)₂] (3, 6) containing the P,O-bound phosphine ligands *i*-Pr₂PCH₂CH₂OMe (1) and *i*-Pr₂PCH₂C(O)OMe (2) have been prepared from [RuCl₂(PPh₃)₃] and 1 or 2 by ligand exchange. Reaction of 3 with carbon monoxide leads to the formation of [RuCl₂(CO)₂(η¹-P-*i*-Pr₂PCH₂CH₂OMe)₂] (4) in nearly quantitative yield. On treatment of 3 and 6 with HC≡CPh or HC≡CCO₂Me, the vinylideneruthenium(II) complexes [RuCl₂(=C=CHPh)(η¹-P-*i*-Pr₂PCH₂CH₂OMe)(η²-*i*-Pr₂PCH₂CH₂OMe)] (5) and [RuCl₂(=C=CHR)(η¹-P-*i*-Pr₂PCH₂C(O)OMe)(η²-*i*-Pr₂PCH₂C(O)OMe)] (7, R = Ph; 8, R = CO₂Me) are formed, which are fluxional in solution. From ³¹P NMR measurements at various temperature, the free enthalpies of activation $\Delta G_{218}{}^* = 41$ kJ/mol for 5, $\Delta G_{275}{}^* = 53$ kJ/mol for 7, and $\Delta G_{258}{}^* = 49$ kJ/mol for 8 for the intramolecular rearrangement have been determined. The X-ray crystal structure analysis of 5 (monoclinic space group $P2_1/c$ with $a = 13.129$ (1) Å, $b = 12.803$ (1) Å, $c = 18.867$ (2) Å, and $\beta = 102.42$ (1)°) reveals that in the solid state one phosphine is coordinated via phosphorus and oxygen forming a five-membered chelate whereas the other phosphine is only P-bound with a dangling CH₂CH₂OMe fragment. The Ru=C=C unit is almost linear with Ru–C and C–C distances of 1.749 (5) and 1.339 (7) Å.

Introduction

During the last decade, the chemistry of vinylidene transition-metal complexes has attracted a great deal of attention.[2,3] Among the metal centers used to bind a C=CRR′ unit, ruthenium plays a prominent role. There are, however, only a few examples of vinylideneruthenium complexes which do not contain a cyclopentadienyl or an arene ring as a supporting ligand.[3,4]

In the present paper we describe the synthesis and structure of ruthenium compounds of general composition [RuCl₂(=C=CHR)L₂] in which L is a potential bidentate but hemilabile chelating ligand. It is shown that in contrast to P-*i*-Pr₃, the related ether and ester phosphines *i*-Pr₂PCH₂CH₂OMe (1) and *i*-Pr₂PCH₂C(O)OMe (2) support the formation of a Ru=C=CHR unit from 1-alkynes

HC≡CR as starting materials.

Results

Preparation of the Ruthenium Complexes 3–5.

Following earlier work from our laboratory in which it was illustrated that the coordinatively unsaturated compound [RhCl(P-*i*-Pr₃)₂]ₙ[5,6] serves as an excellent starting material for the synthesis of vinylidenerhodium(I) complexes,[7] we attempted to prepare an analogous bis(triisopropyl-

(1) Part XIX of the series Vinylidene Transition-Metal Complexes. For part XVIII, see: Werner, H.; Weinand, R.; Knaup, W.; Peters, K.; von Schnering, H. G. *Organometallics* **1991**, *10*, 3967.

(2) (a) Bruce, M. I.; Swincer, A. G. *Adv. Organomet. Chem.* **1983**, *22*, 59. (b) Antonova, A. B.; Johannsson, A. A. *Usp. Khim.* **1989**, *58*, 1197. (c) Werner, H. *Angew. Chem., Int. Ed. Engl.* **1990**, *29*, 1077.

(3) Bruce, M. I. *Chem. Rev.* **1991**, *91*, 197.

(4) Dixneuf, P. H. *Pure Appl. Chem.* **1989**, *61*, 1763.

(5) (a) Preparation in situ: Busetto, C.; D'Alfonso, A.; Maspero, F.; Perego, G.; Zazzetta, A. *J. Chem. Soc., Dalton Trans.* **1977**, 1828. (b) Isolation: Werner, H.; Wolf, J.; Höhn, A. *J. Organomet. Chem.* **1985**, *287*, 395. (c) The compound is monomeric in benzene[6a,b] but dimeric in the solid state.[6c]

(6) (a) Schneider, D. Dissertation, Universität Würzburg, 1991. (b) Schneider, D.; Werner, H. *Angew. Chem., Int. Ed. Engl.* **1991**, *30*, 700. (c) Haas, J. Dissertation, Universität Kaiserslautern, 1990.

(7) (a) Wolf, J.; Werner, H.; Serhadli, O.; Ziegler, M. L. *Angew. Chem., Int. Ed. Engl.* **1983**, *22*, 414. (b) Garcia Alonso, F. J.; Höhn, A.; Wolf, J.; Otto, H.; Werner, H. *Angew. Chem., Int. Ed. Engl.* **1985**, *24*, 406. (c) Werner, H.; Wolf, J.; Garcia Alonso, F. J.; Ziegler, M. L.; Serhadli, O. *J. Organomet. Chem.* **1987**, *336*, 397. (d) Werner, H.; Garcia Alonso, F. J.; Otto, H.; Wolf, J. *Z. Naturforsch., B: Anorg. Chem., Org. Chem.* **1988**, *43*, 722. (e) Werner, H.; Brekau, U. *Z. Naturforsch., B: Anorg. Chem., Org. Chem.* **1989**, *44*, 1438.